C-CORE Publication No. 90-21

ICE SCOURING
AND THE DESIGN
OF OFFSHORE PIPELINES

Calgary, Alberta
Canada

Invited Workshop
April 18-19, 1990

PROCEEDINGS

Sponsored by:

Canada Oil & Gas Lands Administration
(COGLA)

and

Centre for Cold Ocean Resources Engineering
(C-CORE)

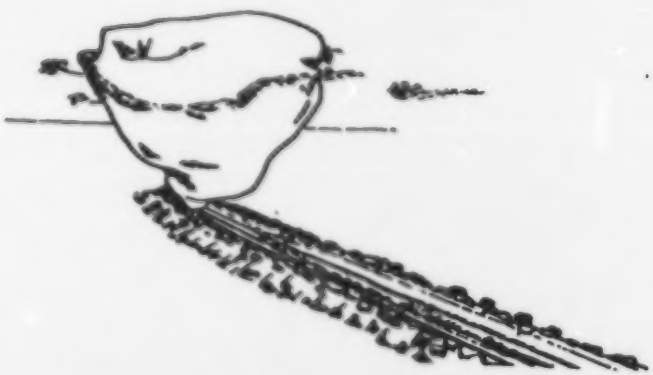

92-01899/

On Small Scale Ice Scour Modelling

F.Poorooshasb and J.I.Clark
Centre for Cold Ocean Resources Engineering
Memorial University of Newfoundland

Abstract

This paper reviews the recent work undertaken by C-CORE on the small scale modelling of ice scour. The results of small scale scours in saturated silt (from the lab and the field) as well as the results of model tests in dry sand are presented. These results pertain to displacements, surface and subscour morphology, and forces on the scouring iceberg. The implications for damage zones associated with scouring are presented. Finally, the difficulties with extrapolating these model tests to the full scale are presented, and means are suggested by which these difficulties may be overcome.

Introduction & Literature Review

The phenomenon of ice scour is a prevalent one in the Canadian offshore and in other ice infested regions (eg. Lewis & Barrie[1981]). Scour occurs when a mass of ice (an iceberg or pressure ridge keel) moves while in contact with the seabed (see figure 1). Scours such as those created by icebergs on the Grand Banks of Newfoundland may be several kilometres in length, and typically have an incision depth of less than 1 metre and a width of between 20 and 40 metres (ibid.). Extreme scour morphology of up to 124 metres in width and 6.5 metres of depth have also been reported. Scour frequencies in different areas have also been calculated, an example being the 4.3% scouring quoted for the Saglek Bank by Woodworth-Lynas et al[1985].

The study of ice scour has been approached from phenomenological, theoretical and experimental points of view. Examples of phenomenological studies include those references quoted above. These studies are the most relevant, because they deal with the full sized, field phenomenon. Unfortunately, these studies yield little or no information about the required driving forces and the sub-seabed processes attendant upon scour, and so can be used only with caution to make predictions.

Many theoretical studies of differing natures have been conducted by various authors to investigate the problem of ice scour, which have yielded theoretical models of the scour process. Examples of these authors include Chari[1979], Palmer et al[1989], Harrison[1982] and Clark & Poorooshasb[1989]. These theoretical models show considerable variation, particularly in the area of the amount of subscour deformation. Much of the discrepancy may be attributed to the fact that the boundary conditions for the full scale problem are not well known or are not fully accounted for in the theoretical models. Two parameters which vary considerably between models include the attack angle (angle which the forward

scouring face of the ice makes with the seabed) and the effect of considering the problem as one in plane strain as opposed to three dimensions.

Small scale physical modelling has been applied to this problem for a considerable period. Harrison[1972] and Chari[1979] based or verified their theoretical models on physical model tests. Abdelnour & Graham[1984] conducted a series of tests at medium scale in the laboratory, as did Poorooshasb[1989] and Poorooshasb et al[1989]. As in the case of the theoretical models, the results of these physical models vary considerably. This, again, is because the physical modelling of the scour process is an idealisation, and so the boundary conditions chosen for the physical modelling will affect the types of results obtained. Important parameters include the ratio of model to container size, the ratio of cut width to depth, the attack angle of the model ice, the degrees of freedom of the ice and the density and physical properties of the soil into which the model ice scours.

This paper addresses some of the most recent modelling conducted by C-CORE at the Memorial University laboratories, and a set of small scale ice scour observations in the St. Lawrence estuary at Montmagny, Quebec. It will discuss how this modelling improves on previous experiments and the conclusions derived from the tests. Finally, the deficiencies of small scale modelling are described, and means by which improved physical modelling may be accomplished are suggested.

Silt Scour Modelling

A pair of tests conducted in a tank of saturated silt in the Memorial University soils lab have been fully reported by Poorooshasb et al[1989]. The main points of the tests will be brought out here, in order to allow comparison with further results and to allow discussion. The silt displayed a shear strength between 4 and 10kPa, as measured by hand vane. A layer of silty clay with a PI of about 8, a shear strength of about 10kPa, and a thickness between 10 and 20mm was present as an overlying layer. Buried in the test bed were 6 pore pressure transducers. In addition, the silt was laminated with tthin layers of fine sand horizontally orientated, created by the process of sediment deposition.

The model iceberg consisted of several aluminum plates welded together to form a complex prism (see figure 2). This model iceberg was designed to be able to move freely in a vertical plane; so as to be able to pitch and to heave. The iceberg was connected to a gantry which spanned the tank and drove the iceberg through the silt. In this test series, the model iceberg was driven forward at a rate of $0.06ms^{-1}$.

The size of the iceberg relative to the silt tank was deemed small enough to cause few boundary effects. The iceberg was 400mm in width, and scoured at (average) depths of 40mm and 70mm (in the two runs). The silt test bed was 3m wide and 0.4m deep, and it was felt that only in the deep scour (70mm) was there any chance of the base of the tank interfering with the experimental results.

Some of the results from these tests are shown in figures 3 to 5. These figures show surface morphology, subsurface deformations as determined from the mapping of the once-horizontal laminations, and pore pressure changes as measured by the pore pressure transducers. The main points are as follows.

The first test, conducted at a cut depth of 40mm, did not break through the clay crust and appeared, from a plan view, to have created little damage (only a polished groove where the iceberg had scoured). Beneath the scour, however, the laminations appeared to have mirrored the surface morphology, down to 5 scour depths (0.2m). Pore pressure response of up to 6kPa also indicated plastic soil reaction at considerable distances away from the scour.

The second test, conducted at a cut depth of 70mm, broke through the plastic clay crust and created a dramatic incision. Large pieces of this crust and the underlying soil were pushed upwards and outwards, in a manner which appeared to be similar to a bulldozing action. Cracks on the surface of the clay appeared, orientated at approximately 45° to the direction of travel. Below the surface, the laminations again showed deformations occurring in a manner which mirrored the surface morphology. However, unlike the case of the shallow scour, the laminations were not traceable below the centre of the deep scour. It was surmised that the deformations underneath the deep scour may have been sufficiently large to have completely remoulded the soil and thus precluded the detection of the fine laminations.

Overall, the results of the silt scours showed that whereas no rupture planes were detected (probably due to the low strength of the silt) data was obtained which indicated deep deformations. It was not possible to ascertain whether the material which was pushed downwards eventually moved forwards and upwards or sideways and upwards.

"Lab In the Field"; Montmagny

The tidal flats in the St. Lawrence estuary show examples of small scale ice scouring, comparable to seabed scour (on a reduced scale). Every year, the St. Lawrence freezes, and a layer of sediment is deposited under the ice cover. This ice cover is of the order of 1 metre thick. As the spring thaw approaches, the ice cover breaks up during the high spring tides. Ice rafting results in numerous small "icebergs" many of which are about 25 tonnes in size. These icebergs are carried away under the action of the river's current and the ebbing tide, often creating small scour marks. Thus, the St. Lawrence Estuary can be considered to be a large "lab in the field".

Tidal flats in the St. Lawrence Estuary have been documented (eg. Dionne[1988]). These flats include the area adjacent to Montmagny, Quebec, where the overlying unit is reported to consist of fresh, soft to firm gray-brown muds (0.1-0.5m), overlying a laminated estuarine light brown mud (1-2.5m), in turn overlying a late-pleistocene light blue marine clay (Dionne[1974]). At the particular sites investigated by the author, the distinctions between units were not so clear, but the top unit appeared to be silt with approximately 10%-15% of clay and sand inclusions, and the second unit was found to be a silty sand (~55% medium to fine sand with a few pieces of gravel). The shear strength of the top unit varied from about 0.5 kPa (essentially too low to measure with a hand held shear vane) to 5kPa; this variation is shown in figures 6. As the second unit was encountered, refusal of the shear vane occurred and so no shear strength values were obtained.

At the above-mentioned site, several fresh scours were found at every low tide (surface evidence of older scours tended to be washed away by each high tide) (see figures 7-8). These scours showed very sharp lineations and polished surfaces. They tended to be formed at a constant depth relative to the horizontal, and did not conform to the topography of the tidal flat. The side berms and end berms were very small, and the ratio of depth to width was also very small (see figure 8). Also, in some cases, the scouring ice mass was observed at the end of the scour track; these ice masses did not seem to have sunk very deeply into the underlying soil (see figure 9).

A site investigation was conducted at 5 scour tracks. In each of these sites, the profile of the scour was measured, and the shear strength variation with depth was measured at intervals of 0.1m (with a hand vane). A trench was then dug across the width of the scour so as to allow a visual examination of the soil. Soil samples were retrieved at various depths, which were later analysed for water content and particle size (see figure 10).

The results of these site investigations proved to be surprising, in light of the small amount of visible surface deformation. Little visual evidence was obtained of shear zones beneath the scours or of deformations of subscour laminations. However, evidence of the deformations was obtained by observing the variation in shear strength. In the areas where shear strength profiles were obtained, such as depicted in figures 6, the contours of strength appear to map with the surface contours. This implies that the subsurface layers are being pushed downwards to mirror the surface displacements. A qualitative assessment of the same can be seen from figure 11, where the interface between two soil layers (a soft layer overlying a stiffer layer) was detected by hand and traced. In this case, it can again be seen that the soft top layer was pushed downwards, which in turn pushed down the stiffer layer below.

Sand Scour Modelling

A series of 4 scour model tests was conducted in the Memorial University sand tank. The purpose of this test series was to investigate the size and nature of the deformation zone below a scouring iceberg, to determine what effect the width and attack angle of the iceberg had on the scour process, and to measure the force vector required to create the scours.

In these tests, the sand-filled area of the tank was 3m wide, 8m long and 0.6m deep. The sand was a clean dry silica sand supplied by Nova Scotia Sand and Gravel (see figure 12). Shear box tests were undertaken to determine the simple behaviour of the sand (see figure 13); it had a residual friction angle of 33°. At high densities (~70% relative density) close to the maxima encountered in this test series, the apparent angle of friction rose to 43° at low stress levels (<50kPa); at stress levels of 100 to 200kPa the dilation was largely suppressed and an angle of friction of 37° was measured. For each test, the soil sample was created by a raining procedure which enabled sand beds to be laid between limits of approximately 0% and 60% relative density. During intervals in the raining procedure, the sand was levelled off by the use of a vacuum cleaner mounted on a gantry, and inclusions

placed within the soil. After the entire bed had been created, it was vacuumed down to the desired height to produce a flat horizontal model soil bed for the tests.

The inclusions which were placed within the soil during the raining intervals were load cells and various displacement markers. The load cells were squat (0.012m diameter by 0.004m tall) cylinders which measured the change in total stress by means of a strain gage bonded to a thin diaphragm. Back-calibrations on the load cells indicated that the stress concentration on these cells was (with one exception) close to unity. The load cells were all orientated so that they measured the total stress change acting on a horizontal plane. Most of the stress cells were placed along the centre line of the scour at differing depths; others were placed at offsets away from the centre line.

The displacement markers consisted of 0.5" steel ball bearings, strands of solder and chains of paper clips. The ball bearings each bore an identification number so that they could be differentiated, and they were laid in a grid pattern in a vertical plane perpendicular to the axis of the scour. The ball positions were determined as they were laid using a pointer system mounted on the overhead gantry. Subsequent to the tests, the sand was removed and the new positions of the displacement markers were obtained. Thus, the before and after records of the ball positions yielded data which could be used to determine total displacement vectors.

The solder and paper clip chains were used to qualitatively display displacements. The use of paper clip chains was discontinued after the first test, because it was seen that the excavation process disturbed the chains. However, the solder was used extensively and did not appear to be disturbed due to the excavation. After the first test, solder was laid at a variety of depths below the surface and offset in the y direction relative to each other, in order to create a "terraced" effect. This terracing yielded a good qualitative picture of the variation in displacement in the y direction with respect to z and x. Due to the inextensibility of the solder, it understated the displacements.

The model icebergs consisted of regular polygons, with vertical side walls, a horizontal base, a vertical rear wall and an angled front face (see figure 14) The model iceberg widths were either 430 or 860 mm, and the attack angle of the front plate was set at either 15° or 30° (the attack angle is here defined as the angle which the front face makes with the horizontal). The model icebergs were made from aluminum alloy, which had an angle of friction of 20° with the sand. Embedded within the angled front face and the horizontal base were pressure cells located flush with the surface, which measured the normal pressures at discrete spots on the iceberg surface. Finally, the iceberg was mounted on a series of struts which drove it horizontally through the soil bed while measuring the vertical and the horizontal forces.

The test parameters are as shown in Table 1. All scours were cut into a soil bed 0.6m thick (ie the surface was at z=0.6m) and the bottom of the model iceberg was at z = 0.525m, so the scour cut depth was 0.075m. The two figures in the relative density column refer to the density of the soil which was encountered first, followed by the density of the soil which was encountered next. These two densities were laid so as to allow the effect of variation of soil type to be determined.

Table 1

Test	Attack Angle/°	Width/mm	Relative Density/%
1	15	430	8 / 36
2	15	860	8 / 29
3	30	860	-2 / 46
4	15	860	60 / 18

It should be pointed out that the relative density measured in this test series displayed greater variation than was hoped, and so the above numbers represent an average value across the thickness of the sample. A variation of up to 10% was not uncommon.

Typical examples of the results from this test series are as shown in figures 15 to 22. These figures include records of total horizontal and vertical forces during a test run, spot pressures on the iceberg attack face and the horizontal base, displacements as indicated by solder strands and the steel balls buried in the sand, the direction and line of action of the resultant force on the iceberg, and photographs of the scour from the surface and during the excavation.

From the surface, the scour tracks which were created appeared similar to those which are detected on the seabed. As the model iceberg advanced into the soil, a berm built up ahead of it. At the same time, rupture planes surfaced ahead and to the side of the iceberg, with rigid blocks of sand moving out of the way of the advancing iceberg. In the looser sands, the rupture planes were numerous and the blocks of material were small; in the denser sands, the rupture planes were much rarer, but were associated with larger movements of large blocks of sand. In addition, the rupture planes surfaced ahead of the berm forward of the iceberg; it appeared that as this forward berm enlarged, so too the foremost rupture plane moved further forward relative to the iceberg.

An interesting anomaly appeared as the model iceberg approached the end of the soil bed. The forward rupture plane, rather than appearing at the horizontal surface of the sand, appeared on the downward sloping end of the soil model, at a depth estimated at 0.15m. This implies a plunging rupture surface which was attracted to a weak material zone (ie air). This situation may be analogous to the approach of a scouring iceberg to an infilled trench.

Two factors have been shown by this test series to significantly affect the amount of subscour deformation. The first factor is that of soil density. Figure 18 shows the results of the solder strand deformations in test 4. The figure is a plan view of the test bed after the scour, in which the iceberg advanced from right to left (ie it travelled along the y axis, in the direction of decreasing y). The dotted line labelled "Iceberg Edge" represents the track of the outside edge of the model iceberg. The curved lines crossing the model scour represent the deformed shape of the solder strands after the scour. The strands on the right of the figure represent those strands laid in dense soil (60% RD) and those at the left were laid in looser soil (18% RD).

The first point which can be seen is that in the dense soil, the zone in which

deformations occurred was restricted to immediately below the iceberg scour. At z=0.52m (0.005m below the scour), the solder strand was broken and the edges swept parallel to the iceberg track. However, 0.02m below this (and further below, but not shown on this diagram) no deformations were observed in the solder strands. This indicates that a zone of material exists below the scouring iceberg in which the soil moves with the iceberg and severe displacements occur, and that this zone is limited to the near-field of the iceberg. However, in the case of the looser soil, deformations were observed down to a depth of z=0.46m, or 0.065m below the scouring model. Thus, in looser soils, the zone of deformation underneath a scour is much greater, and the amount of deformation reduces as the iceberg is distanced.

The type of deformations underneath the looser sand should be noted. It can be seen that the strand at z=0.48m has a central portion, 0.3m long, which has translated "rigidly" in the y-decreasing direction. At a depth of z=0.46, the central portion is 0.17m long, but it has still displaced rigidly by approximately the same amount (0.17m cf 0.14m) as the strand above it. Thus it appears that there may be a zone below the iceberg which exhibits rigid body translation, surrounded by zones which exhibit a considerable degree of shear. It should be pointed out that this behaviour was only seen strongly in the test 4 looser soil, and evidence of this behaviour from the other tests is limited.

The second factor which affected subscour damage was that of attack angle. The two attack angles (of 15° and 30°) showed significantly differing results. Tests 3 and 4 were two tests similar except for the attack angle of the iceberg. However, reference to figures 23 show that in the case of test 3, very little subscour disturbance was detected, and this was limited to a zone very close to the underside of the model iceberg. The lack of deformation was evident in the looser as well as the dense sand. As consideration of figure 23 will show, the displacements are almost entirely in the y direction, with little movement in the z or x directions (vertical or sideways).

The effect of these two parameters upon forces is also evident. The table below summarises some of the force results from the four tests in the series. The figures from test 1 were corrected to take account of the fact that the scour in test 1 was only half of the size created in the other tests.

Table 2

Test	$F_{v\,pk}$	$F_{h\,pk}$	θ_{dense}	$F_{v\,loose}$	$F_{h\,loose}$	θ_{loose}
1	6.5	5	50	2.5	2	50
$1_{(corr)}$	13	10	50	5	4	50
2	9	8	49	7.25	6.5	48
3	7.5	8.5	41	2.25	2.75	40
4	12.5	9.5	51	8.5	7.5	49

In the above table, $F_{v\,pk}$ and $F_{h\,pk}$ represent the peak vertical and horizontal forces measured in the test, θ represents the angle of the resultant force (in the

loose and the dense sand), and $F_{v\ loose}$ and $F_{h\ loose}$ represent the average vertical and horizontal stresses in the looser soil. The peak values of force are quoted rather than the average forces in the denser soils, as an average force in a dilatant rupturing soil would be subjective.

The immediate difference which can be seen from table 2 is that test 3 was an anomalous test, and that the change in attack angle has changed the relative magnitudes of the forces as well as the absolute values. Test 3 was the only test in which the horizontal force was larger than the vertical force.

Beyond this, it is difficult to make firm statements regarding the magnitudes of the forces. Once the correction factor has been applied, it appears that the peak forces measured in tests 1 and 4 coincide very well. However, when the difference in RD of the sands is considered (35% cf 60%) this correspondence should not be so close. Due to the discrepancies in relative density between samples, the closest correspondence should be between the dense sand in test 2 and the loose sand in test 4, and the loose sands in tests 1 and 2. The first correspondence set is surprisingly good (both in terms of magnitude of forces and θ) but the second set is not nearly so.

A further point which has arisen from the force data is that of the change of the resultant angle of the forces; in three out of the four tests, the angle is higher (ie the force was more vertical) for the denser sand.

The pressure sensors located in the faces of the iceberg yielded information regarding the distribution of stresses on the iceberg. Table 3 summarises the maximum stresses measured at the different sites, where σ_n refers to the maximum stress recorded at point n. The coordinate system and point positions are as shown in figure 24. In test 1, the total width of the iceberg was 430mm (so the edge of the iceberg would have a k coordinate of 215mm), and in the latter three tests the edge of the iceberg occurred at k = 430mm. The k_e / k_{edge} column is included to indicate how close to the edge of the iceberg position e is. A value of 1 means that the position is at the edge. The Z_c/Z_d column refers to the ratio of the height below the top of the berm of the points c and d (assuming that the top of the berm coincides with the top of the iceberg), and the σ_c/σ_d column refers to the ratio of stresses at these two points.

Table 3

Test	σ_a (kPa)	σ_b (kPa)	σ_c (kPa)	σ_d (kPa)	σ_e (kPa)	k_e / k_{edge}	Z_c/Z_d	σ_c/σ_d
1	10	18	120	50	90	0.65	1.52	2.4
2	5	10	50	20	50	0.37	3.1	2.5
3	5	0	75	35	75	0.35	1.52	2.1
4	3	3	45	38	59	0.35	1.52	1.2

The most obvious feature here is that the stress levels from points A and B (located behind the inflexion line, on the horizontal base of the iceberg) are very small compared with points C, D and E. This implies that almost all of the force which is applied to the model iceberg arises from the frontal attack plate.

Consideration of points C, D and E indicates that the stress level just forward of the inflexion line is higher than that which is found further forward along the inflexion plate. The last two columns show the relation between depth ratios and stress ratios for points C and D; these ratios can be seen to be within 30% of each other. In addition, in test 1, where point E is close to the edge ($k_e / k_{edge} = 0.65$) the stress level at point E is significantly lower than at point D. However, in the other three tests, the stress level at these two points are similar.

The implications from these stress distributions are as follows. It appears that the normal stress level acting on the attack face of the iceberg is related to the depth below surface of the relevant point on the attack face, but the relationship is not directly proportional to the depth. The stress levels appear to be fairly constant across the central portion of the attack face of the iceberg, but falls off towards the edges. Finally, there appears to be only insignificant stresses acting on the flat base of the model iceberg, implying that this portion of the iceberg has little to do with any failure processes.

The latter tests in this series also yielded data regarding the total stress changes in the soil. A typical record is as in figure 25, where the total stress is seen to dip with the approach of the model iceberg, then rise sharply, and then drop again to give a steady state stress change. A summary of the total stress records is shown below, where the depth refers to the depth below the bottom of the scour and the offset refers to the offset from the centreline of the scour.

Table 4

Test	ID	Density (kgm^{-3})	Stress Dip (kPa)	Stress Rise (kPa)	Stress Change (kPa)	Depth (mm)	Offset (mm)
3	O	1350	0	5	-1.8	70	4
4	A	1420	0	9	-1	40	-3
4	C	1420	0	9	1	60	-442
3	A	1500	-1.5	9	-1.8	125	-6
3	C	1500	-2	5	-1.5	75	-5
4	O	1550	-5	14	-8	120	-10
4	D	1550	-1	15	-1.5	75	-57

All of the results with the exception of instrument 4A and 4C show a stress drop of about 1-2 kPa after the passage of the model iceberg. This corresponds fairly well with the expected drop in total stress due to the removal of 0.075 m of sand. Instrument 4C shows a rise of 1 kPa, which also corresponds well with the creation of a 0.08m berm on top of the instrument. Only test 4O, therefore, can be said to show anomalous results, which is a common problem with total stress cells due to stress concentrations.

The stress dip is present only in the denser sands. This suggests a theory for the means of failure of the soil. As the model iceberg approaches a point, it displaces soil masses. In the dense soils, this results in a rigid block of material sliding upwards along a shear plane. The shear stresses along this shear plane act in an upwards sense upon the soil which is not shearing, ie the soil further ahead of the model iceberg. The upward shear stresses act to reduce the vertical total stress, and so the dip in stress is seen. As soon as the shear planes move forward to include or overlie the sensor, the measured stress level will rise.

This phenomenon is not observed in the looser sands. A possible reason for this is that the soil does not move upwards, but gets pushed sideways or forwards instead. It is difficult to envision no rise, however. Another possible reason could be that the advancing berm (and increase in stress due to it) counteracts the decrease in stress due to rising soil zones. This would imply that the failure regions in loose soils are much closer to the model iceberg.

An interesting comparison is that of the magnitude of the stress increases on the total stress cells compared with those measured on the face of the iceberg. In test 3, for example, the peak stress measured just in front of the inflexion line was 75 kPa. However, the time at which the front of the iceberg was just above sensors A and C was 100s, at which point the stress on the iceberg face was about 40 kPa (it remained at roughly this value from 95s to 110s). The maximum total stress rise observed in the soil was 9 kPa. Since the 40 kPa was measured on a face at 15° to the horizontal, and the principal effective stress occurred on a plane at 40° to the horizontal, the vertical stress at the face was 32.4 kPa. At a depth equal to one scour depth below the iceberg, this stress had reduced by a factor of about 3. Thus, it can be seen that stress levels drop off rapidly below a scouring iceberg.

Summary of Results

The above series of tests bring out several immediate points. These can be summarized as follows:

1) Under certain conditions, significant subscour deformations occur in model tests in fine and in coarse materials.
2) In coarse materials, the deformations are largest in loose soils.
3) In coarse materials, the effect of reducing the attack angle is to increase the force required for scouring and to increase the amount of subscour deformation.
4) In coarse materials, low strength zones appear to attract deformations.
5) In medium to dense sands, the vertical total stress decreases and then increases during the approach of an iceberg.
6) The stress levels fall off rapidly as the distance beneath a scouring iceberg increases in coarse materials.
7) In low strength fine materials, shear strains are set up by the passage of a model iceberg at up to 7 times the scour depth.
8) In fine materials, small surface deformations may coincide with significant subscour deformations.

Point #1 is the most important of these points, in that it states that a dangerous situation may exist for a certain set of boundary and material conditions, without specifying fully what these conditions may be. The other points attempt to specify under what conditions the damage may be significant.

Quality of Results and Means of Improvement

The sets of results obtained from the experiments described above are some of the best sets of modelling results which have been obtained to date. The materials used in the lab tests were well controlled (saturated silt, controlled density sands) and the large scale of the experiments tended to improve the correspondence between the models and the prototypes. The data retrieved from the tests were often part of redundant sets (for example, ball displacement data as well as solder strand data represent the same phenomena). Also, the Montmagny data represents a "half-way house between lab and field scale", and acted to tie the lab results more strongly to the full scale phenomenon.

Quantification of these results and direct extrapolation to the full scale event is difficult because the scaling laws are unclear. In the case of the silt bed, the shear strength of the soil was of the order of 4kPa. If this is used to model sediments of 200kPa strength, then a scaling factor of 50 should be used, implying damage at depths of up to 10 metres. The damaging iceberg would have a width of 20m, a scour cut depth of 2m and a speed of 0.42m/s, which is reasonable. This extent of damage also agrees with the observed field results reported by Woodworth-Lynas and Guigne[in press].

In all three sets of reported data stress and strength varied with depth. If

scour is considered to be a surface phenomenon, then this variation can safely be neglected. However, the results from these tests have indicated that scouring is not necessarily a surface event, but rather extends several metres (at prototype scale) into the seabed. As such, modelling which does not account for this must of necessity be flawed.

These difficulties could be circumvented by use of centrifuge testing of the scour phenomenon. Centrifuge modelling is a technique whereby the centripetal acceleration created by the rotation of a centrifuge is used to model the earth's gravitational acceleration, as is described in greater detail by Schofield[1980]. Essentially, if a model built at a linear scale of N (with all linear dimensions in the model N times smaller than in the prototype) is placed in an acceleration field of N gravities, then the stresses due to gravity within the model will be identical to those experienced by the prototype at full scale. If care is taken to ensure that the boundary stresses are also identical to the prototype stresses, and the model is built of the same material as the prototype, then the model interior stresses and strains will correspond with the prototype, and identical behaviour will ensue. With careful regard to boundary conditions, centrifuge modelling of geotechnical phenomena can yield good quantitative results directly applicable to the prototype.

A typical series of centrifuge tests could be conducted to investigate the effects of scour in both sand and clay. In one scenario, the soil bed would be of the order of 1m by 1m in plan and 0.2m deep. It would be run at 100 gravities, which would therefore model a prototype soil sample 100m by 100m by 20m deep. The soil would either be a clay or a sand; different stress states and histories could be imposed upon these soils to model particular prototypes. The model iceberg would be mounted on a rail overlying the model seabed (see figure 26); it would be driven through the soil at a constant speed and the forces and point stresses acting upon it would be measured. Markers within the soil would yield information on the magnitude of the deformations and the displacement patterns.

The centrifuge experiments are somewhat similar to those conducted in the Memorial University sand tank at 1 gravity. However, there are two crucial differences arising from the increased gravity environment in which the experiments are being conducted. The first is that there is no question as to what scale the experiments are conducted at, ie the magnitude of the prototype iceberg is fully determined by the gravitational scaling factor. Secondly, the modelling of the soil is not affected by differing stress levels between model and prototype, so that it can truly be known what prototype soil (and hence which real geographical areas) is being modelled.

Conclusions

Laboratory and small scale field studies of the scour phenomenon have shown varying degrees of surface and subsurface damage. The damage has, in the worst cases, been shown to extend up to seven times the depth of a scour in fine grained soils, and up to the depth of the scour below a scour bottom in coarse grained soils. In sands, the deformations increase with decreasing attack angle and density. The limitations of small scale scour tests are associated with the difficulty of

extrapolating the results to the full scale and the lack of a correct self-weight stress variation. These difficulties could be circumvented by the use of centrifuge modelling of scour, which would enable soils at prototype stress levels to be tested.

Acknowledgements

The above work owes to considerable effort on many of our C-CORE in colleagues. In particular, Chris Woodworth-Lynas, Jacques Guigne, Don Cameron and Bruce Cole are to be thanked. NSERC provide funding which supported the silt bed modelling and the Montmagny work. The sand modelling was made possible by funding from COGLA and Fleet Technology Ltd.

Bibliography

Abdelnour, R. & Graham, B. "Small Scale Tests of Sea Bottom Ice Scouring", Proc. IAHR, Hamburg, FRG, 1984

Chari, T.R. "Geotechnical Aspects of Iceberg Scours on Ocean Floors", Canadian Geotechnical Journal, Vol. 16, 1979

Clark, J.I. & Poorooshasb, F. "Protection of Sea Bottom Facilities in an Ice Scoured Environment", Proc. Canadian Soc. Civil Engineers, St. John's, NF, Vol iv, June 1989

Dionne, J.C. "Polished and Striated Mud Surfaces in the St. Lawrence Tidal Flats, Quebec", Canadian Jrnl. of Earth Sciences, Vol. 11, No. 6, pp. 860-866, 1974

Dionne, J.C. "Characteristic Features of Modern Tidal Flats in Cold Regions", in Tide Influenced Sedimentary Environments and Facies, eds P.L.de Boer, pp. 301-332, 1988

Harrison, W.L. "Soil Failure Under Inclined Loads", US Army CRREL, DA Project 1T062112A130, Hanover, NH, 1972

Lewis, C.F.M. & Barrie, J.V. "Geological evidence of iceberg groundings and related seafllor processes in the Hibernia Discovery area of Grand Bank, Newfoundland" in Proc. Symp. Production and Transportation Systems for the Hibernia Discovery, W.E.Russell and D.B.Muggeridge (eds.), Newfoundland and Labrador Petroleum Directorate, St. John's, NF.146-177

Palmer, A.C., Konuk, I., Love, J., Been, K., Comfort, G. "Ice Scouring Mechanisms", POAC 89, Lulea, Sweden, June 1989

Poorooshasb, F. "Large Scale Laboratory Tests of Seabed Scour", Contract Report for Fleet Technology Ltd., C-CORE Contract Number 89-C15

Poorooshasb, F., Clark, J.I., Woodworth-Lynas, C.M.T. "Small Scale Modelling of Iceberg Scouring of the Seabed", POAC 89, Lulea, Sweden, June 1989

Schofield, A.N. "Cambridge Centrifuge Operations", Geotechnique 30, 1980

Woodworth-Lynas, C.M.T. & Guigne, J.Y. "Iceberg Scours in the Geological Record" in Glacimarine Environments: Processes and Sediments, Dowdeswell, J. & Scourse, J.D., eds., in press

Woodworth-Lynas, C.M.T., Simms, A., Randell, C.M. "Iceberg Grounding and Scouring on the Labrador Continental Shelf", Cold Regions Science and

Technology, Vol. 10, pp. 163-186, 1985

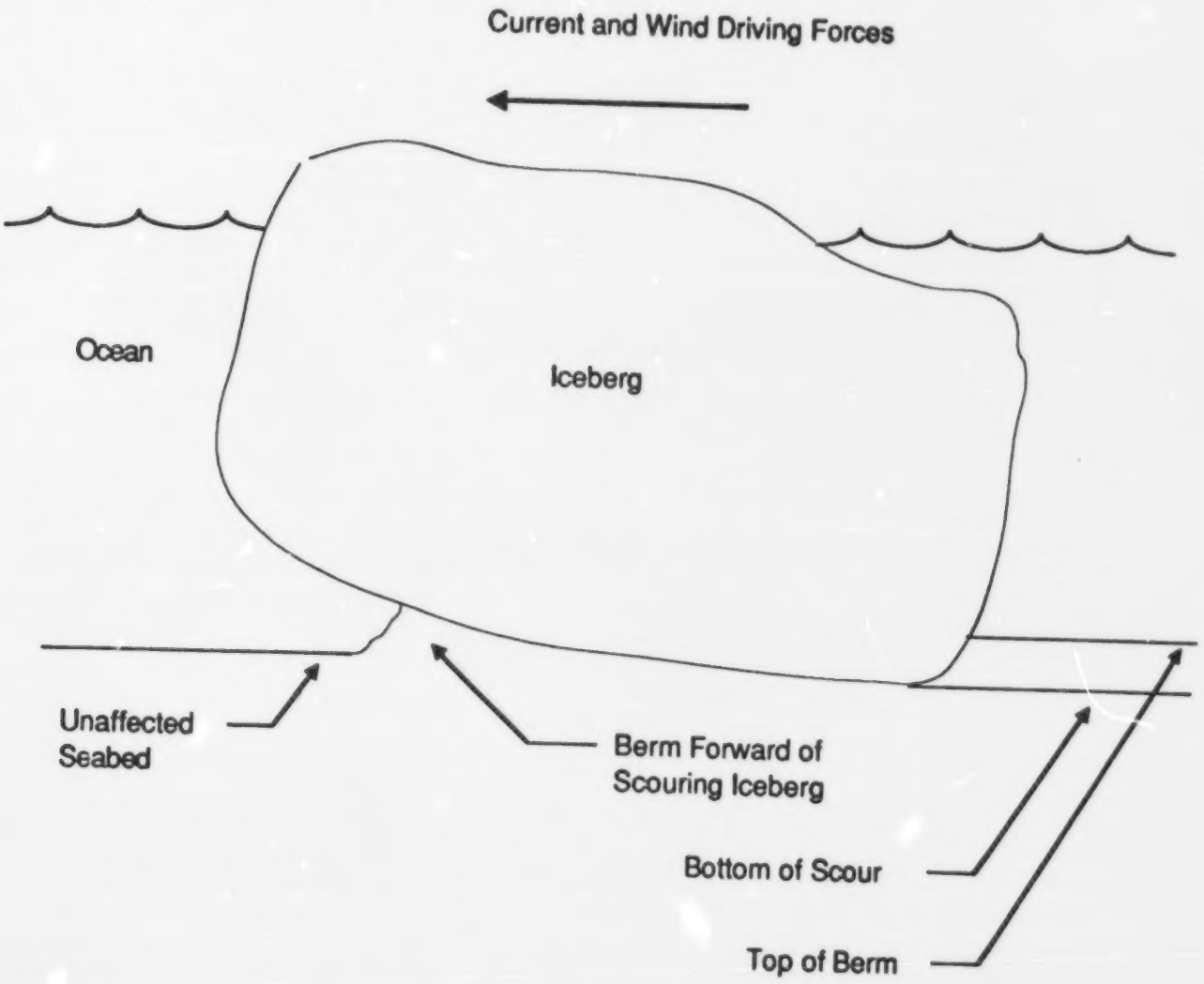

Figure 1
A Scouring Iceberg

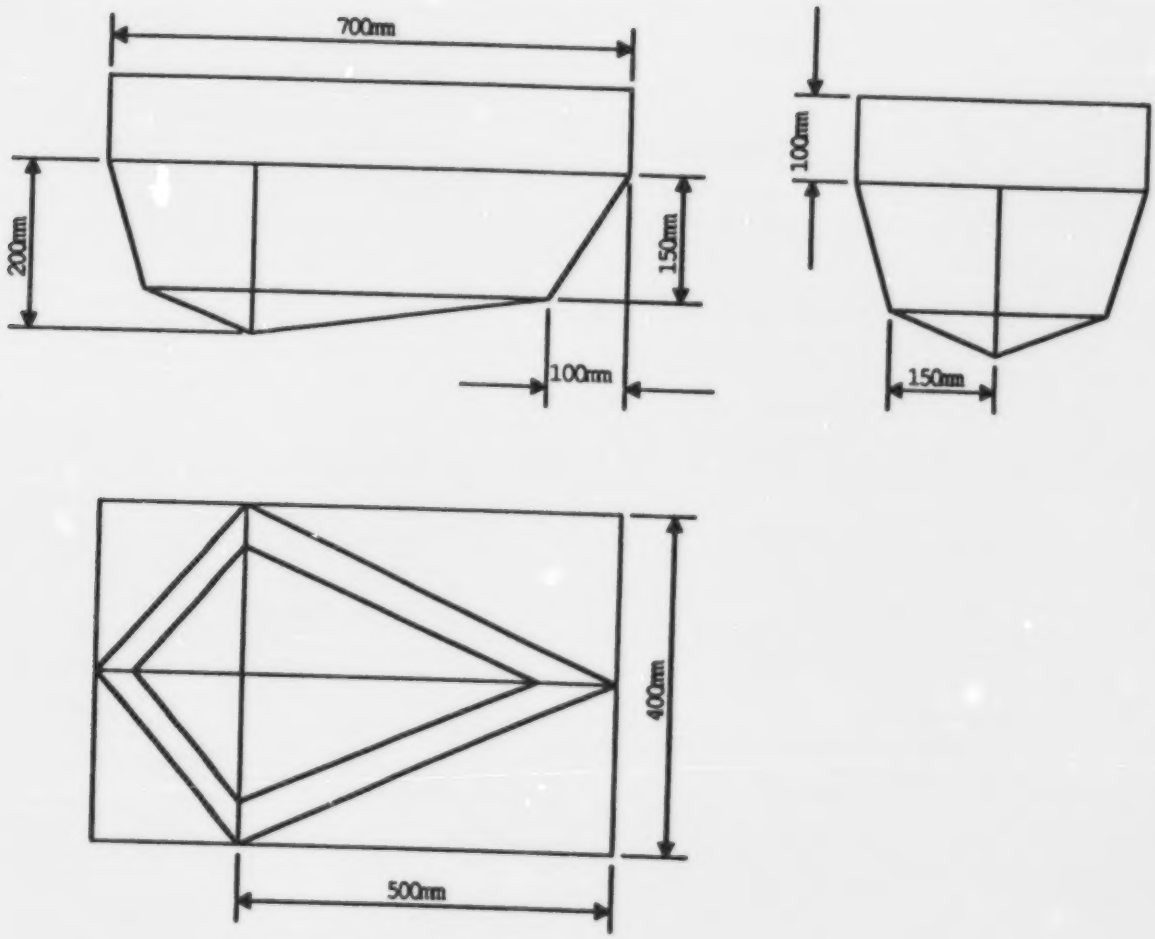

Figure 2
The Iceberg Used in the Silt Tank

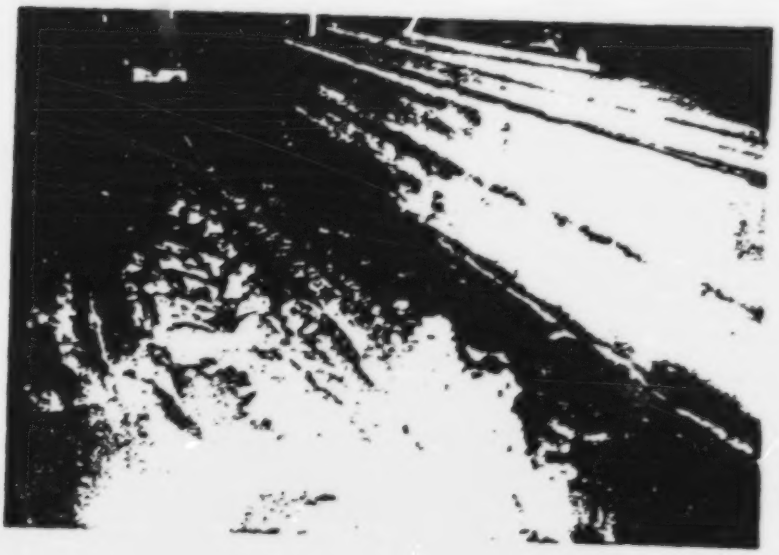

Figure 3
Surface Morphology of Shallow and Deep Scours In Silt

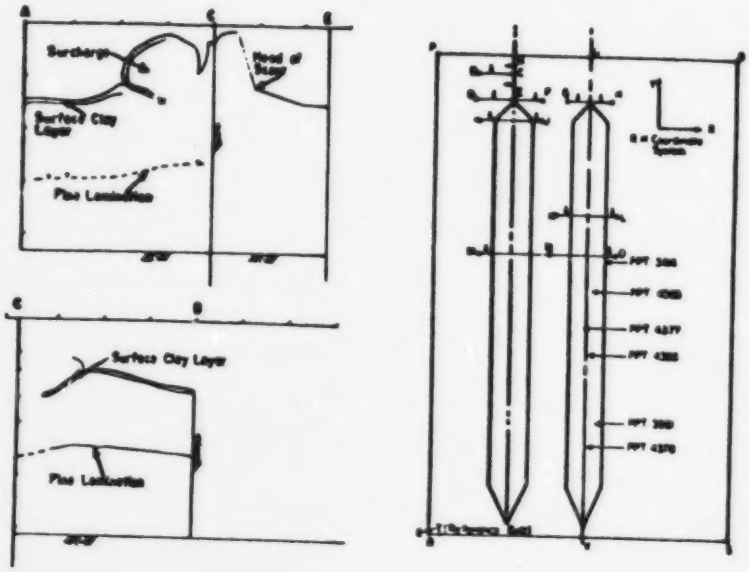

POINT	X	Y	Z
A	-0.72	6.47	
B	-1.10	6.35	
C	-0.72	6.35	
D	-1.12	6.08	
E	-0.72	6.08	
F		6.08	
G		6.08	
H		6.08	
I	-1.42	5.86	
J		5.86	
K		5.00	
L		5.00	
M		4.60	
N		4.60	
O		4.60	
P	-1.42	7.02	
Q	1.42	7.02	
R	-1.42	2.00	
S	1.42	2.00	
T	-1.43	2.00	1.00
U	0.00		
V	0.00	2.00	
3414	0.20	4.60	0.22
4365	0.15	4.30	0.01
4377	-0.01	3.95	0.26
4386	0.03	3.70	0.12
3901	0.15	3.08	0.25
4378	0.05	2.83	0.19

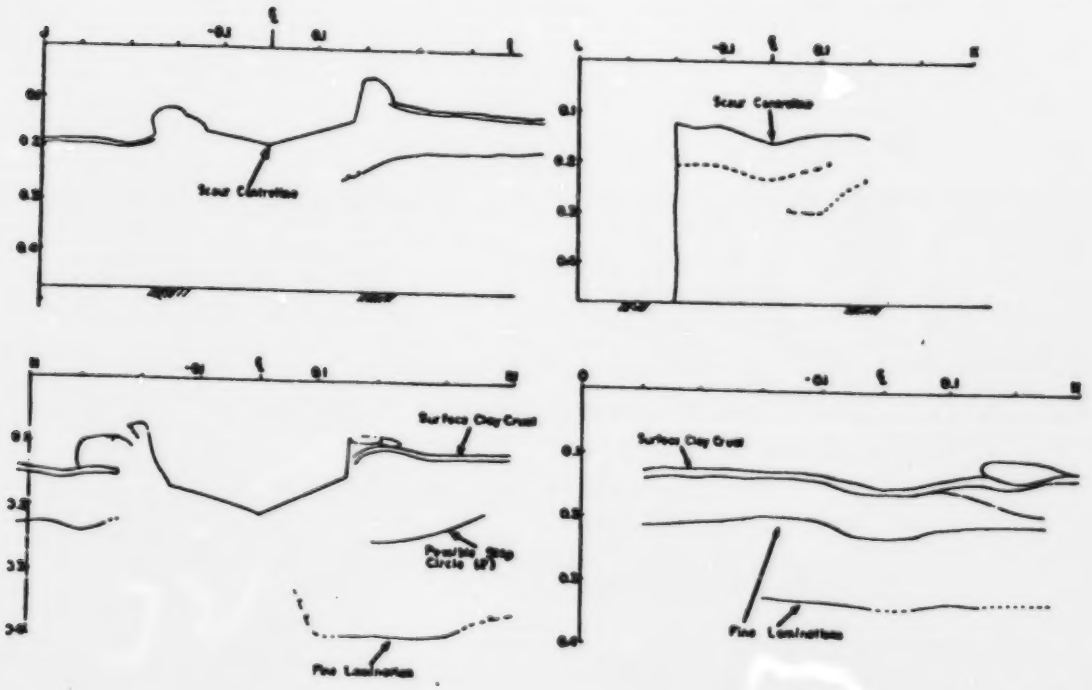

Figure 4
Subsurface Deformations Underneath Scour in Silt Tank

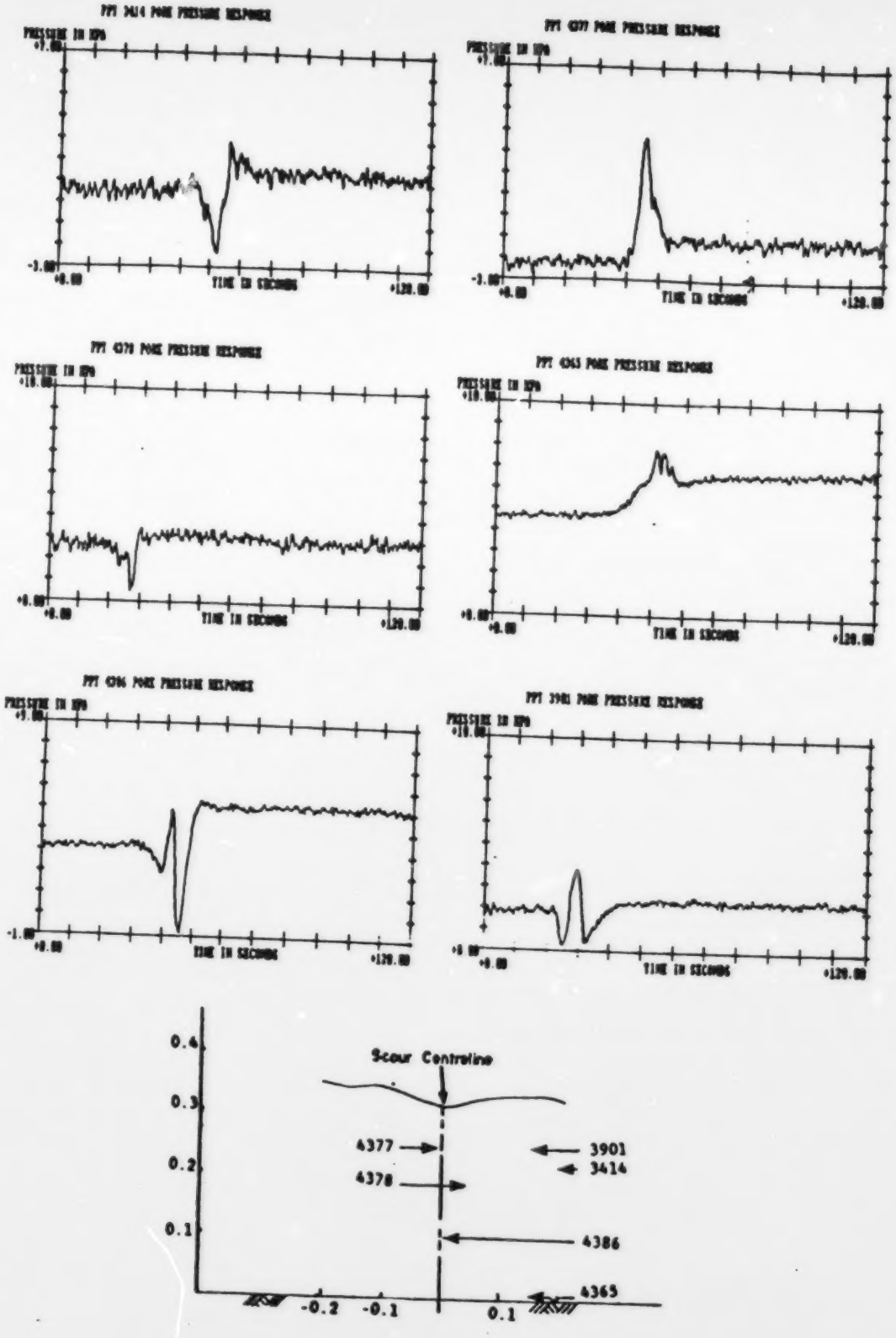

Figure 5
Pore Pressure Changes In Vicinity of Scour In Silt Tank

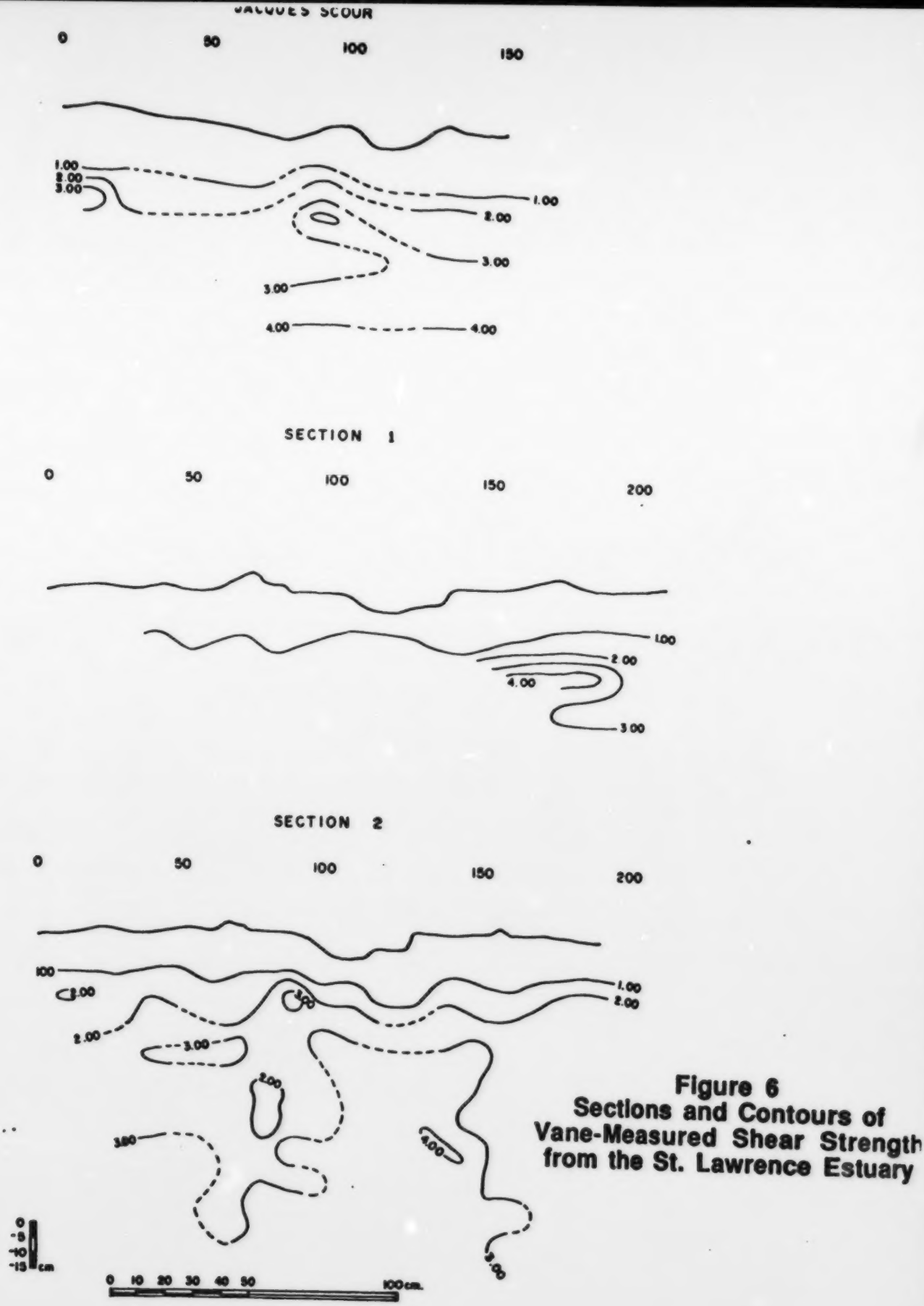

Figure 6
Sections and Contours of Vane-Measured Shear Strength from the St. Lawrence Estuary

Figure 7
Aerial Photograph of St. Lawrence Estuary
During Spring Breakup

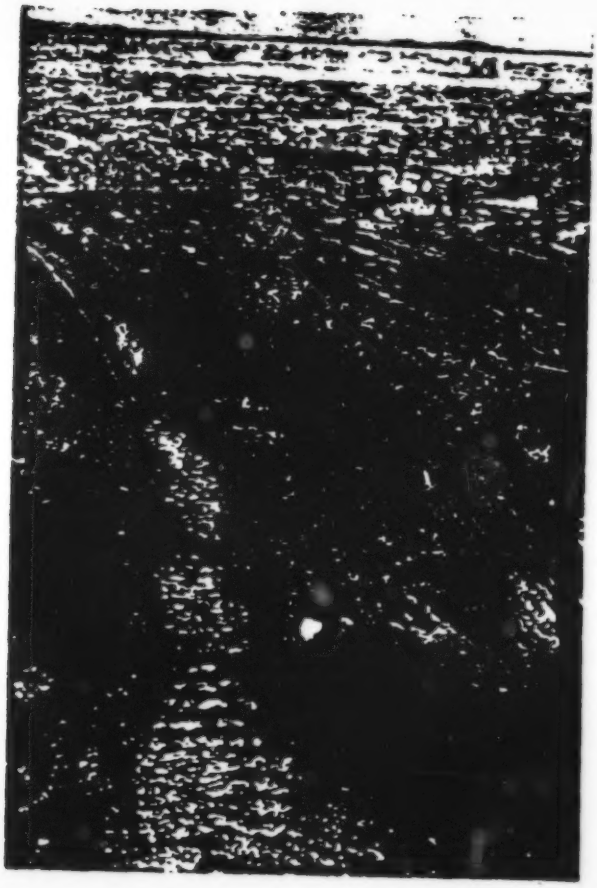

Figure 8
A Typical Scour In the St. Lawrence

Figure 9
A Large Mass of Ice After Coming to Rest

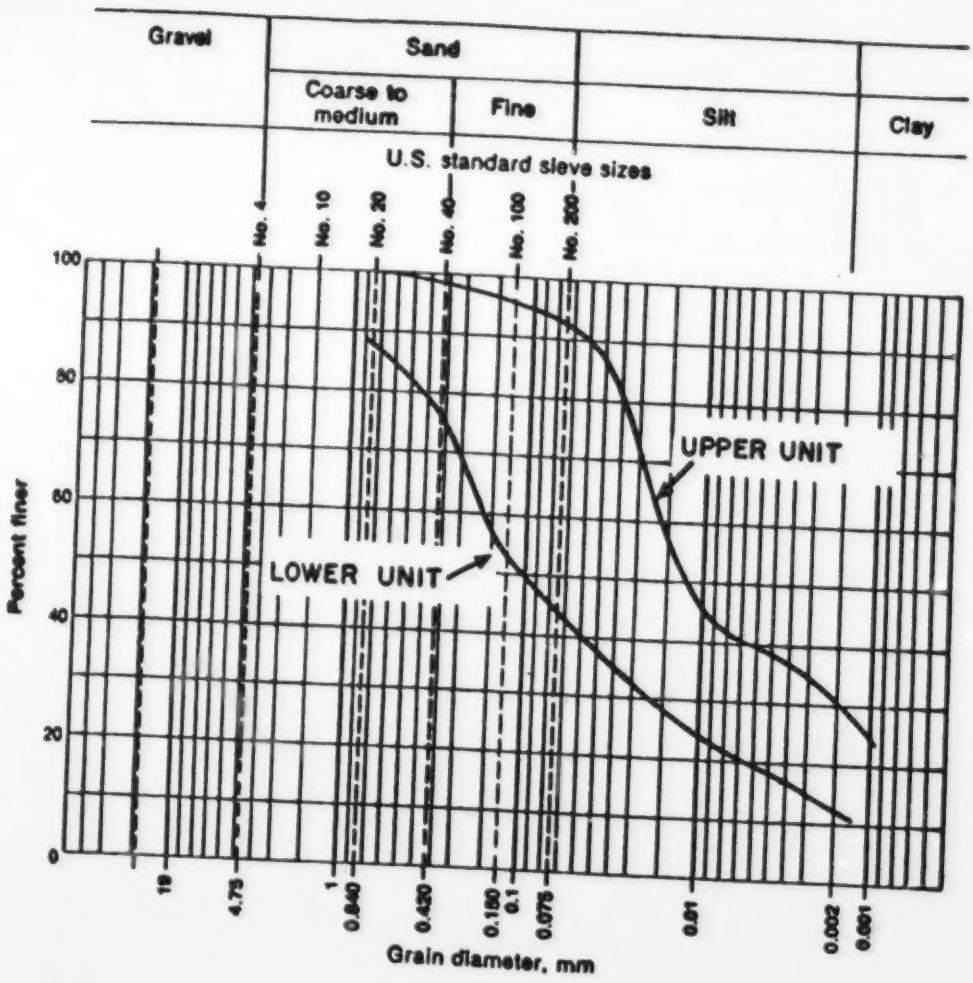

Figure 10
Grain Size Analysis of St. Lawrence Estuary Sediments

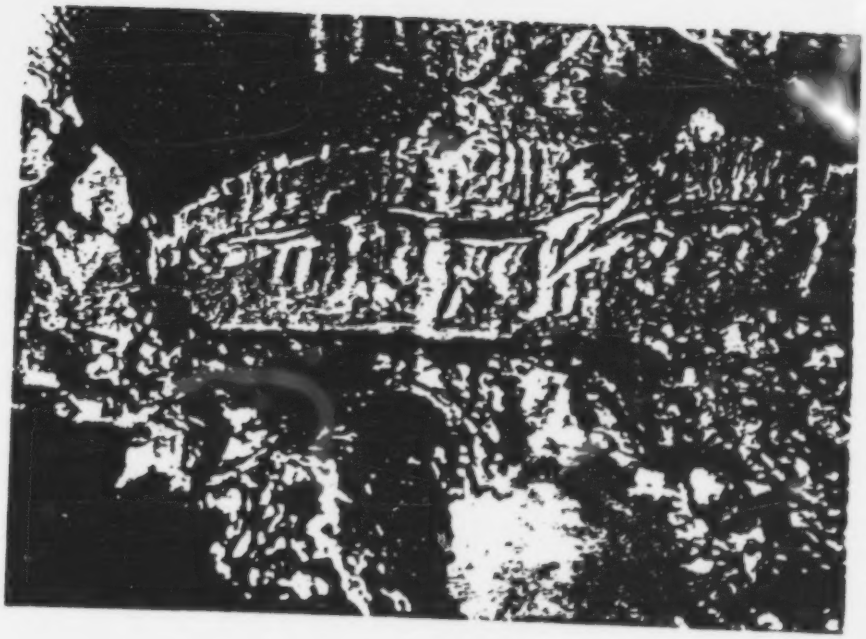

Figure 11
Interface Between Two Layers of Different Strengths on Cross Section of Montmagny Scour

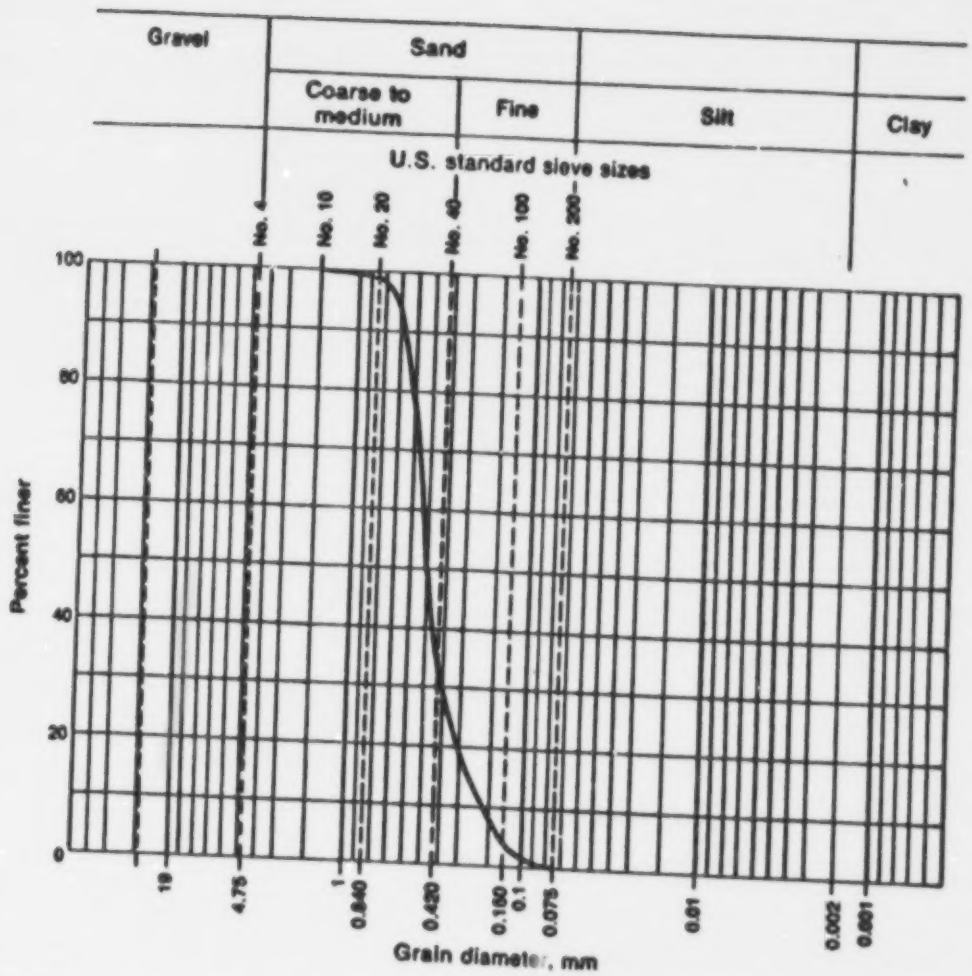

Figure 12
Grain Size Analysis of Sand Used in Model Tests

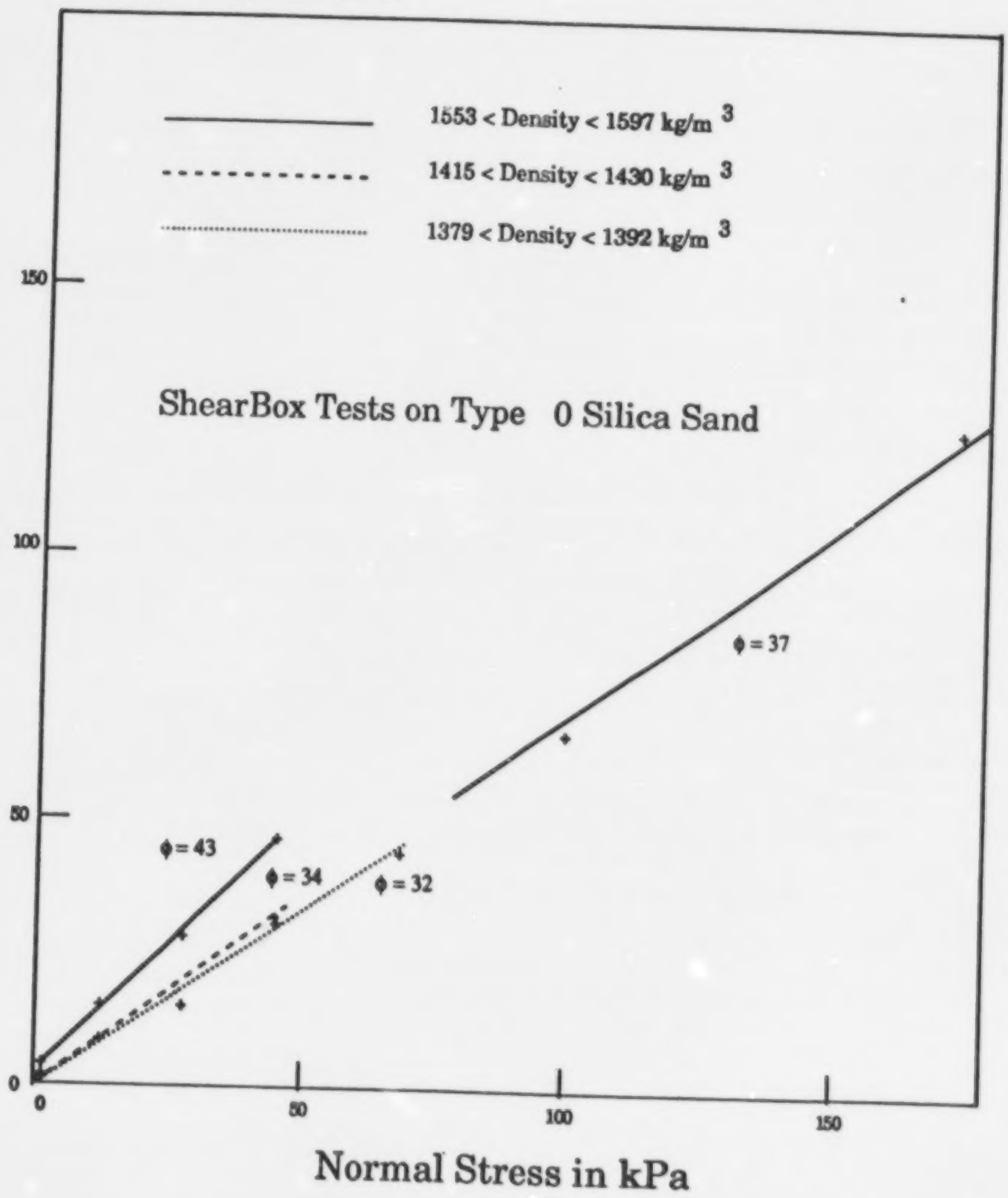

Figure 13
Shear Box Tests of Type 0 Silica Sand

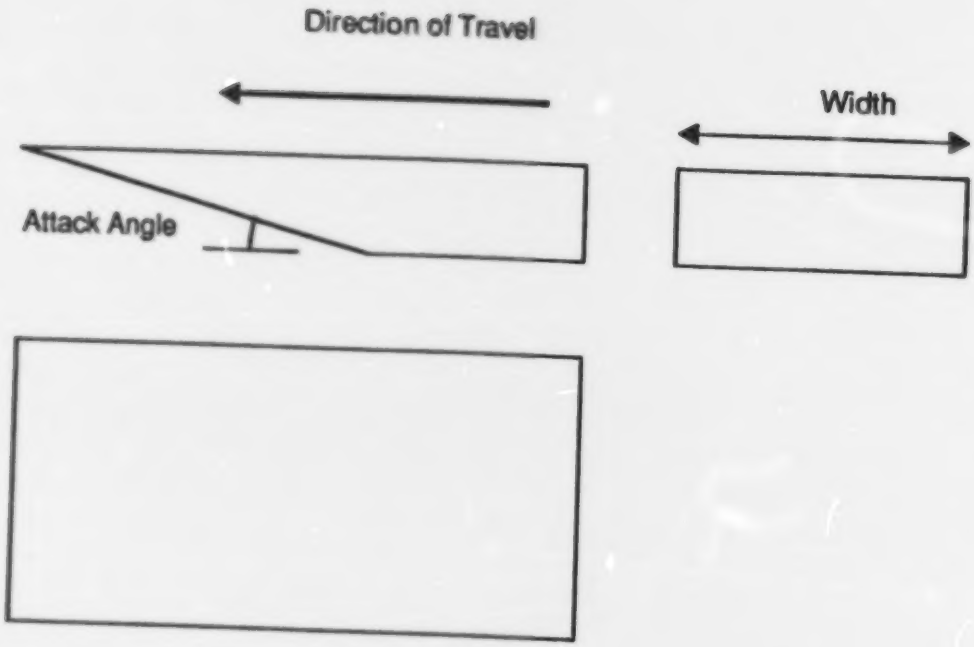

Figure 14
The Model Iceberg Used in the Sand Tests

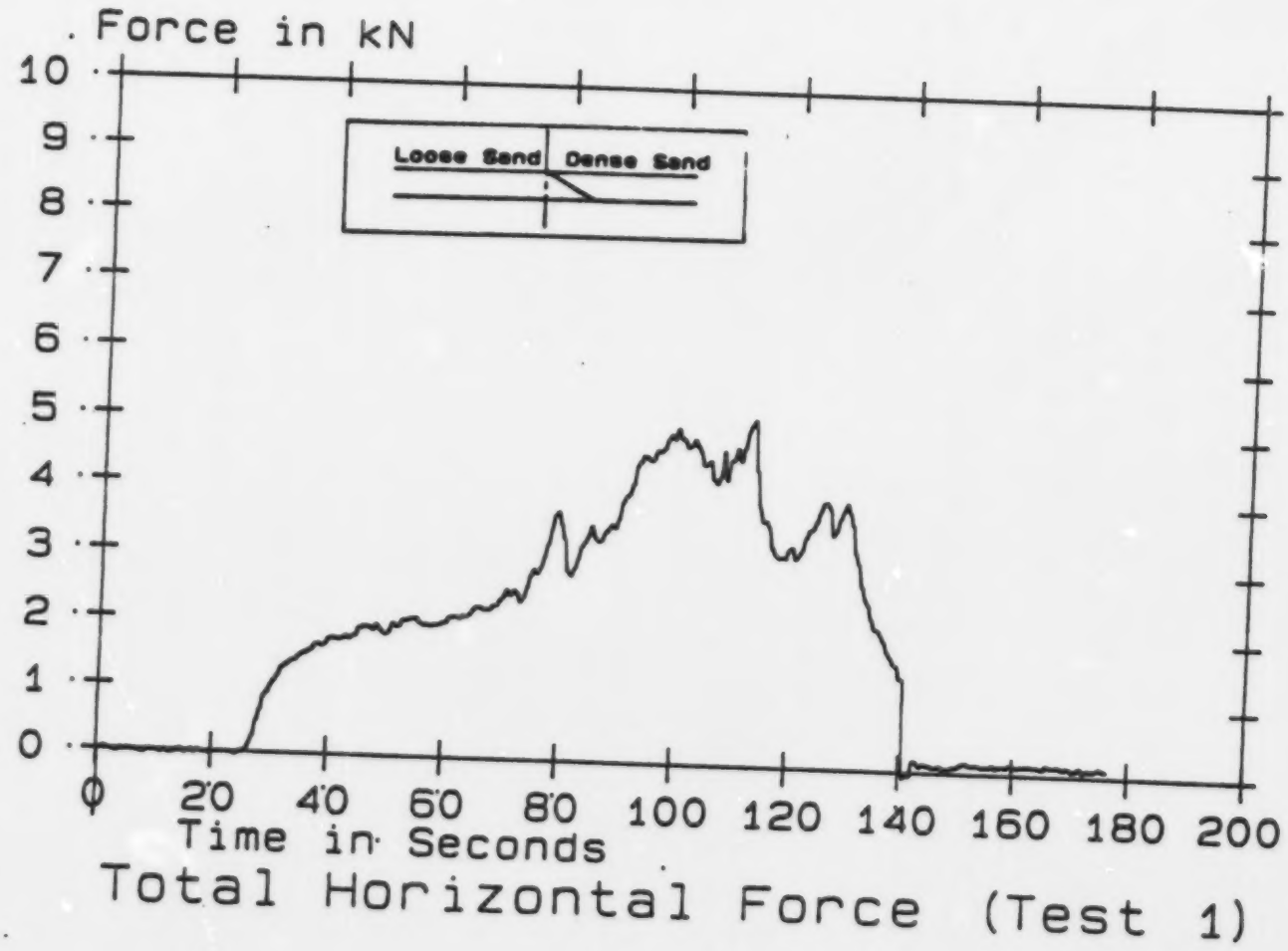
Force in kN
10
9
8
7
6
5
4
3
2
1
0
Loose Sand
Dense Sand
0
20
40
60
80
100
120
140
160
180
200
Time in Seconds
Total Horizontal Force (Test 1)

Figure 15

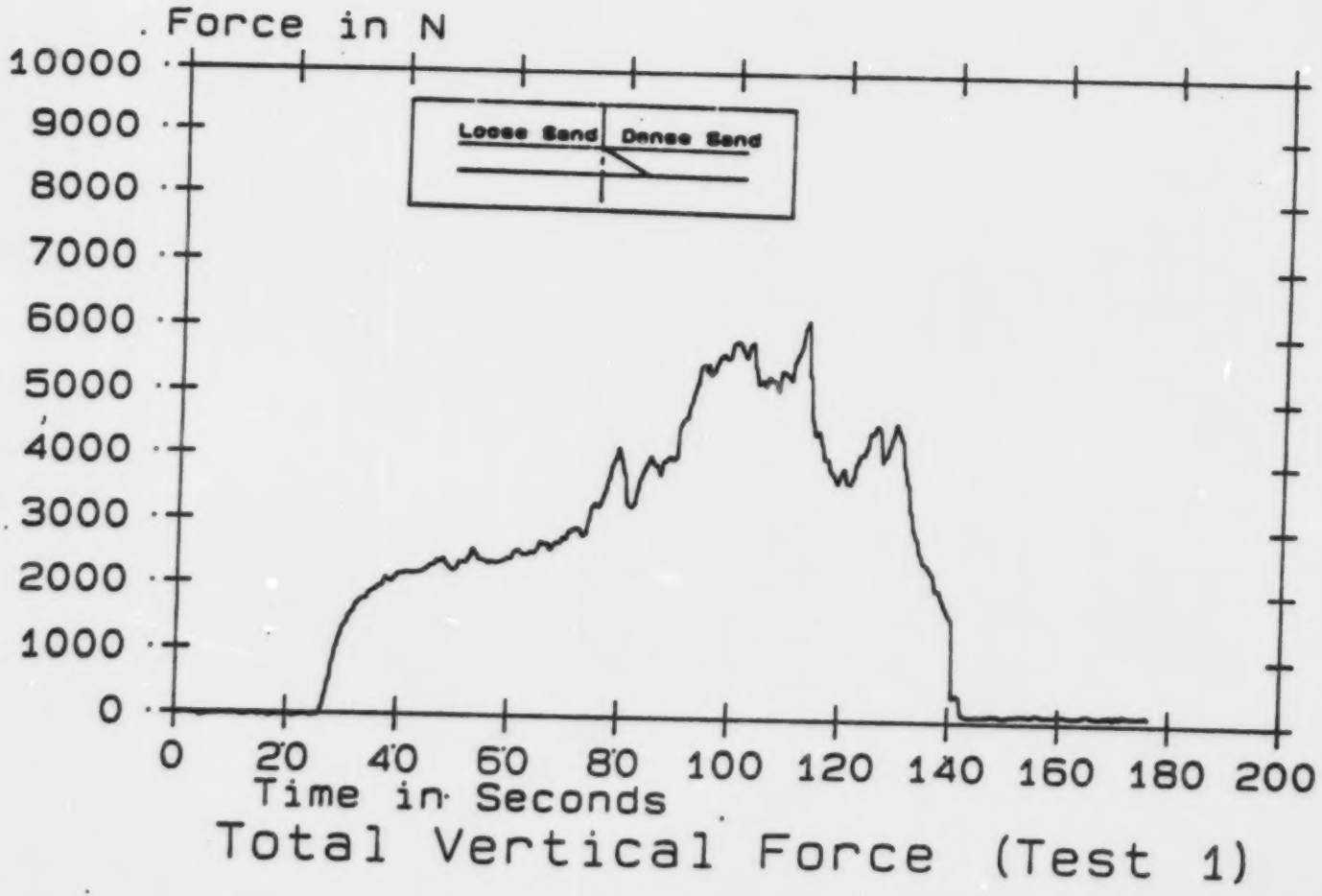
Force in N
10000
9000
8000
7000
6000
5000
4000
3000
2000
1000
0
Loose Sand
Dense Sand
0
20
40
60
80
100
120
140
160
180
200
Time in Seconds
Total Vertical Force (Test 1)

Figure 16

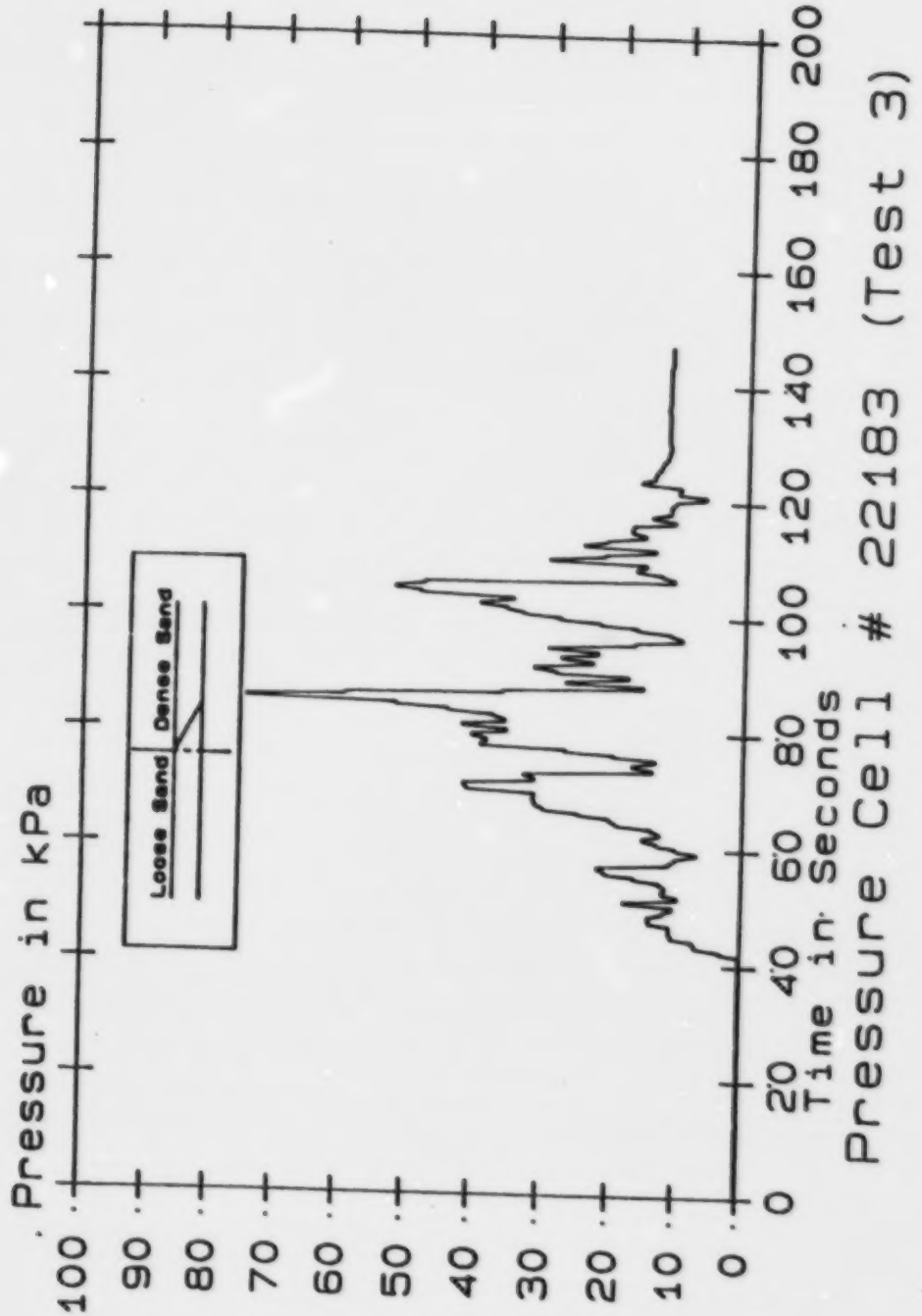

Figure 17a
Pressure Cell Located Just Forward of the Inflexion Line

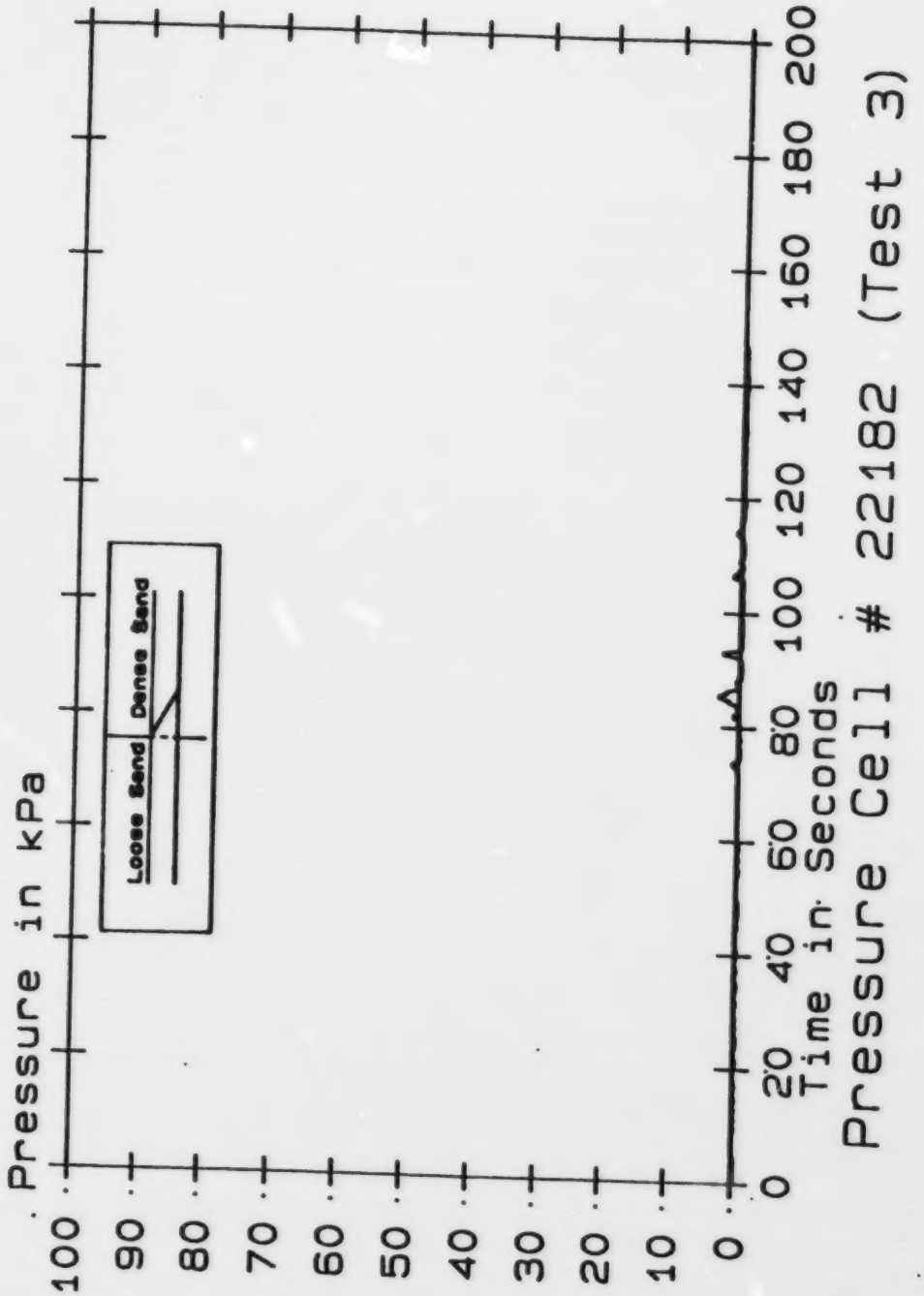

Figure 17b
Pressure Cell Located Behind the Inflexion Line

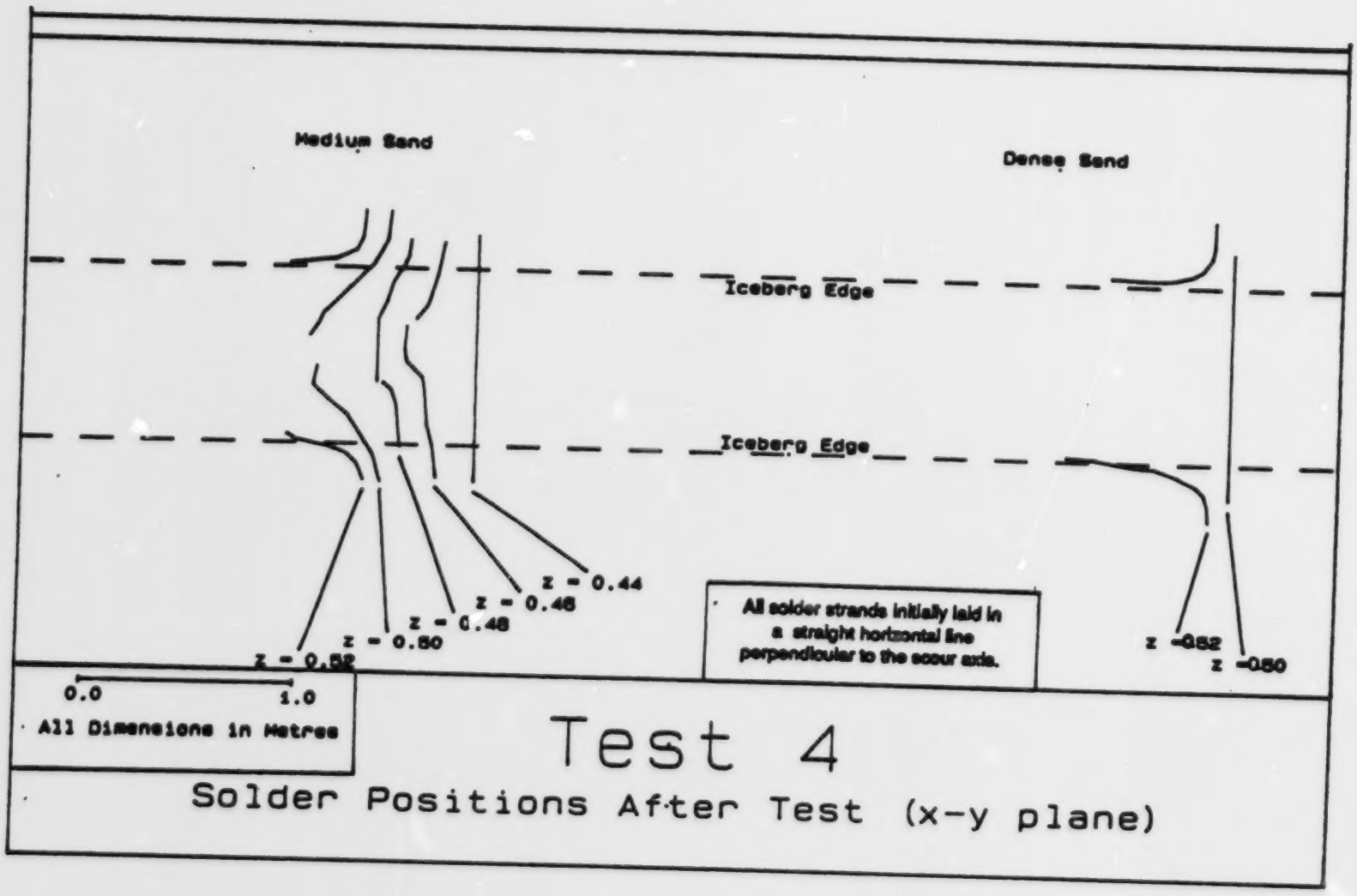

Figure 18
Plan View

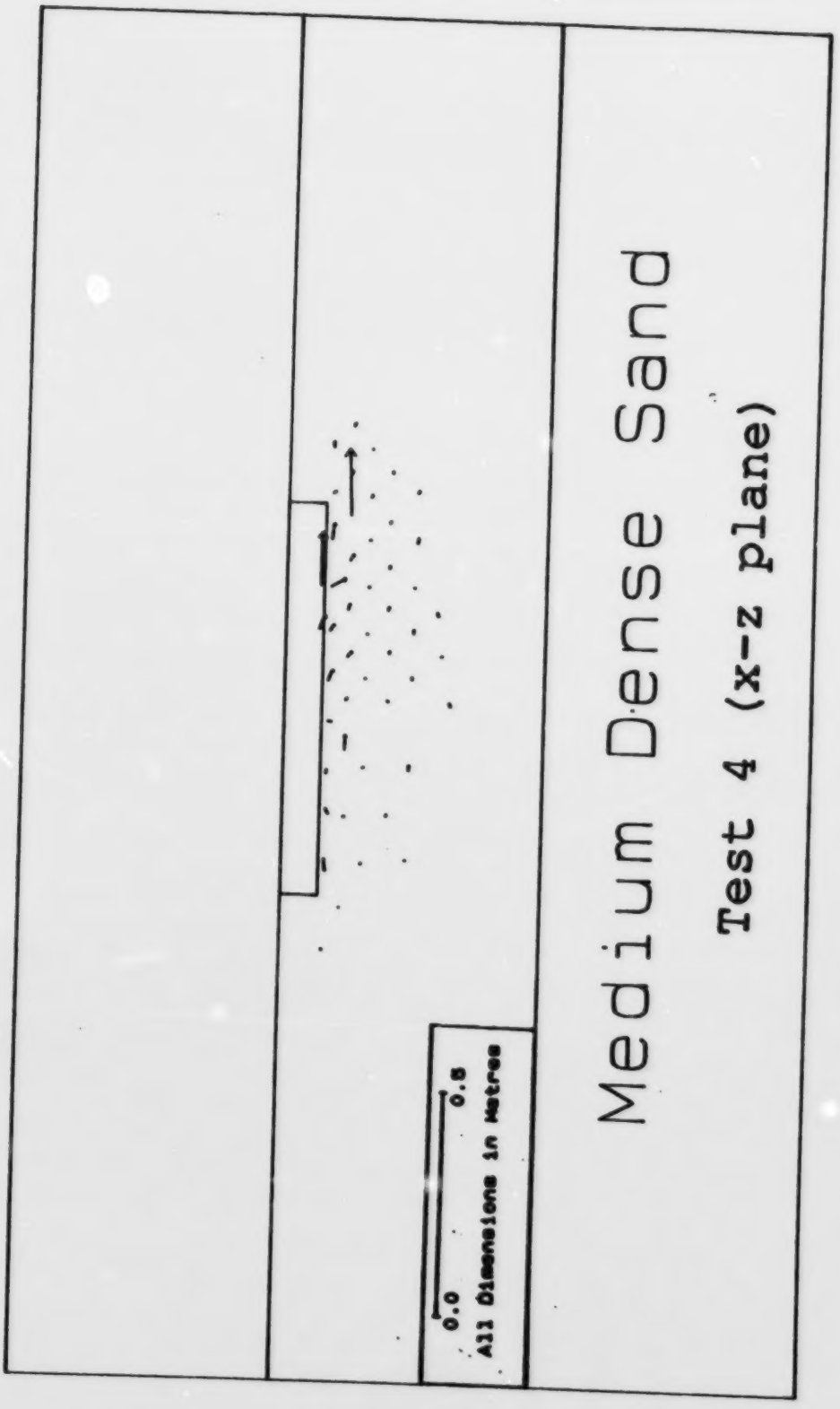

Figure 19a
Ball Displacements, Cross Sectional View
Scour Created Perpendicular to Page

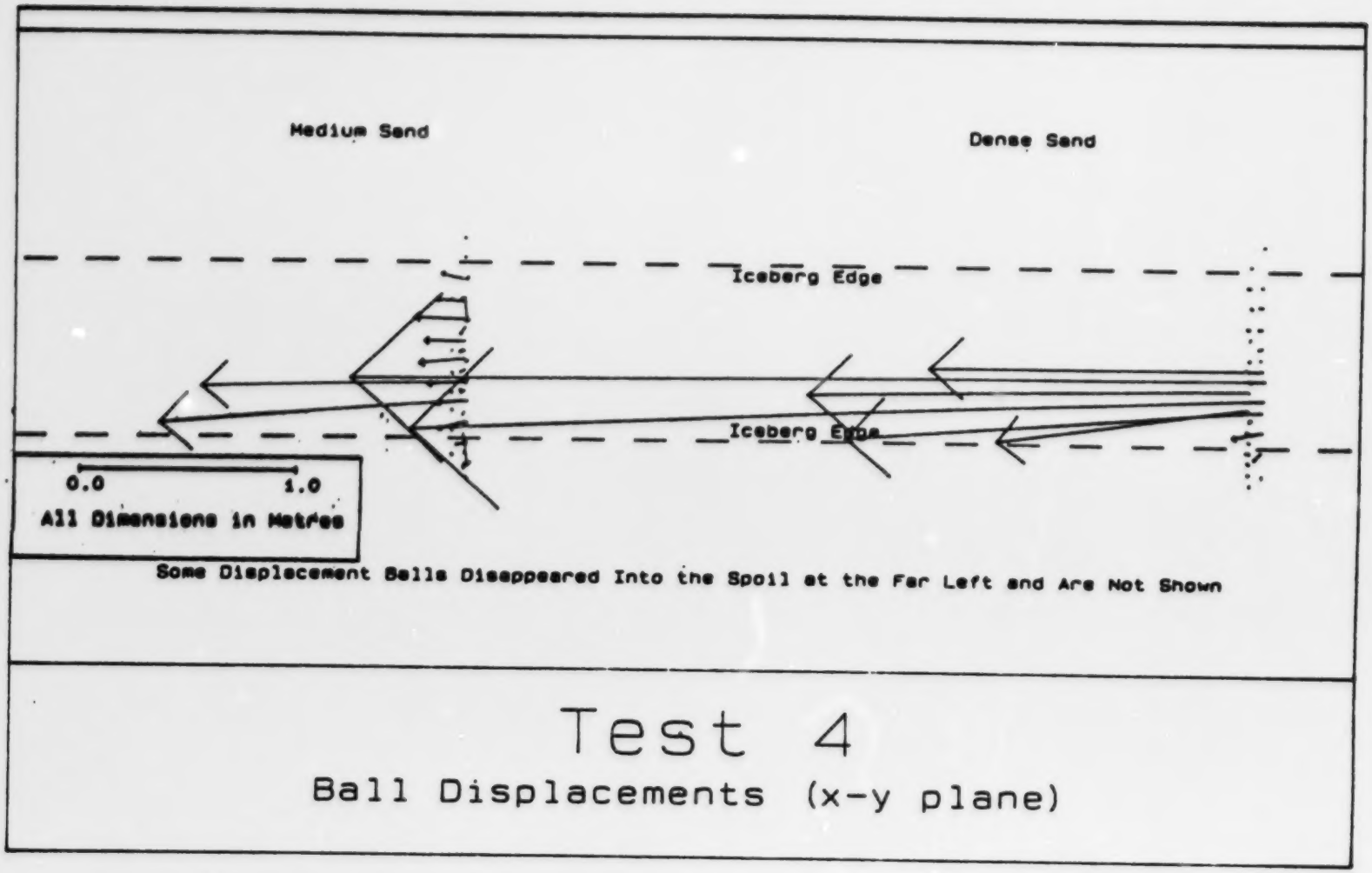

Figure 19b
Plan View
Scour Created from Right to Left

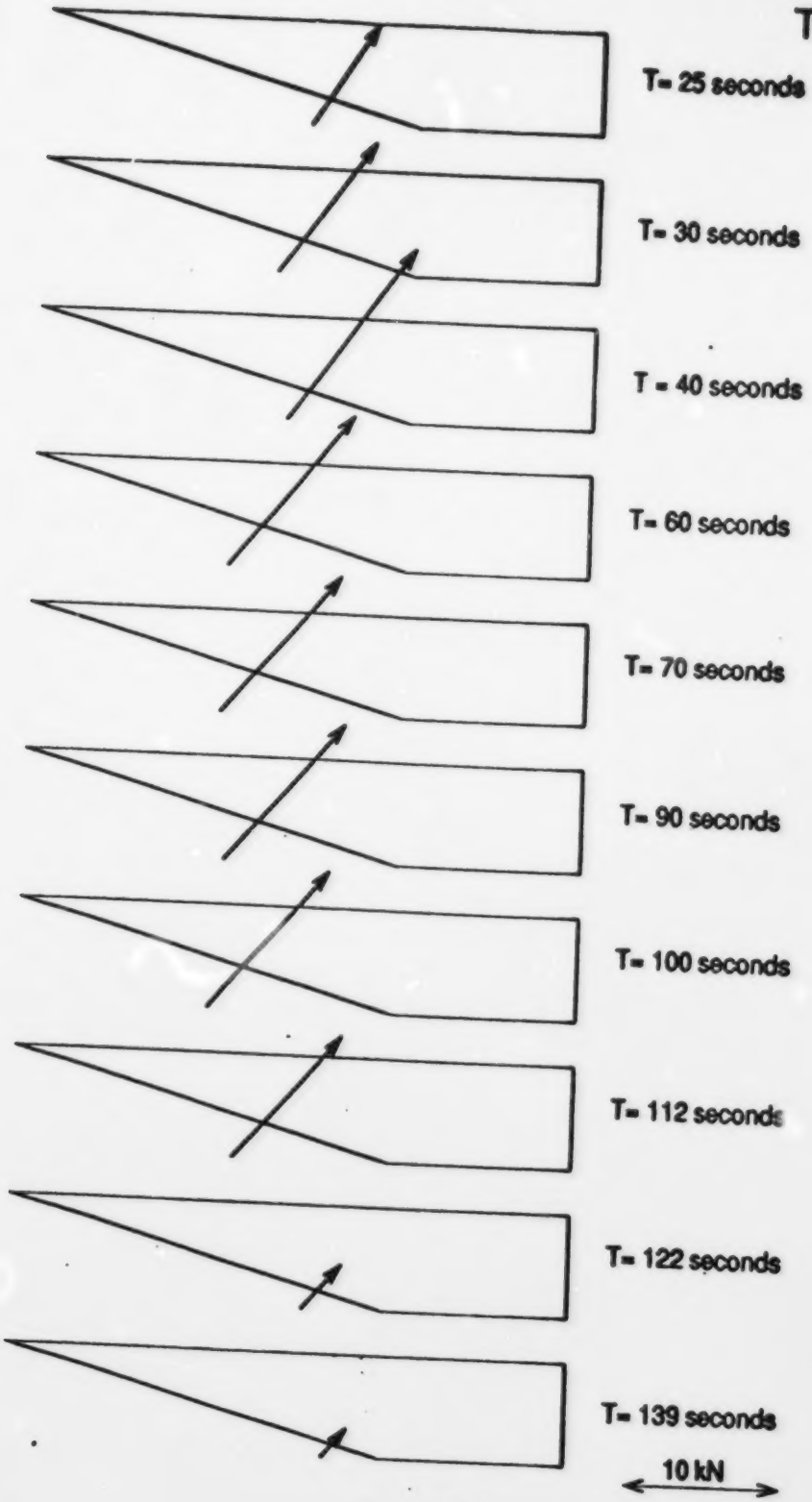

Figure 20
Total Force Vectors

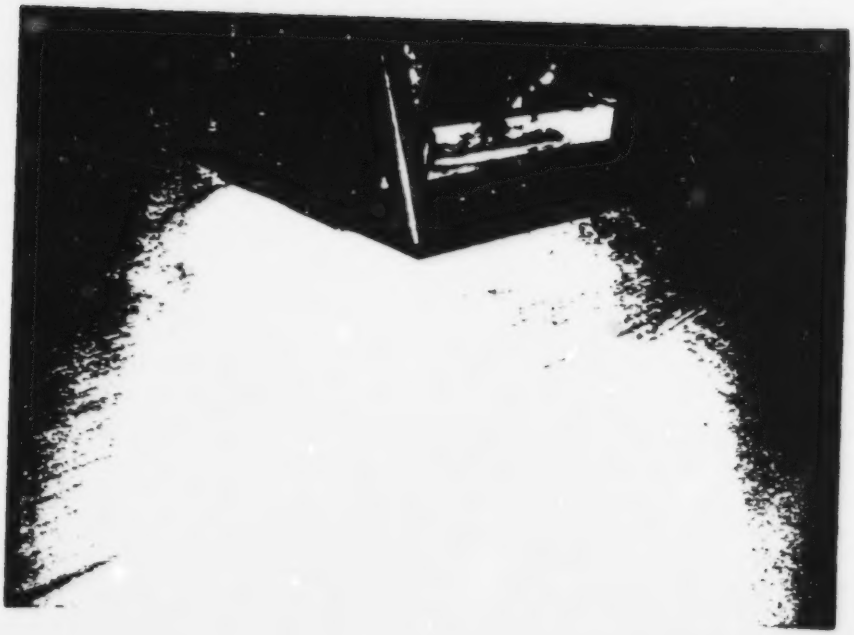

Figure 21
Creation of Scour in Test 1

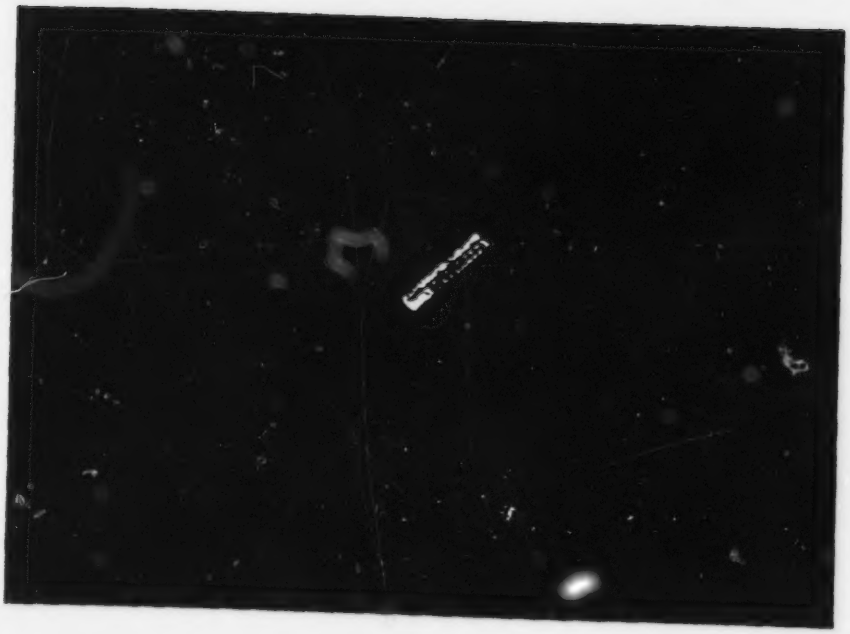

Figure 22
Excavation of Scour in Test 2

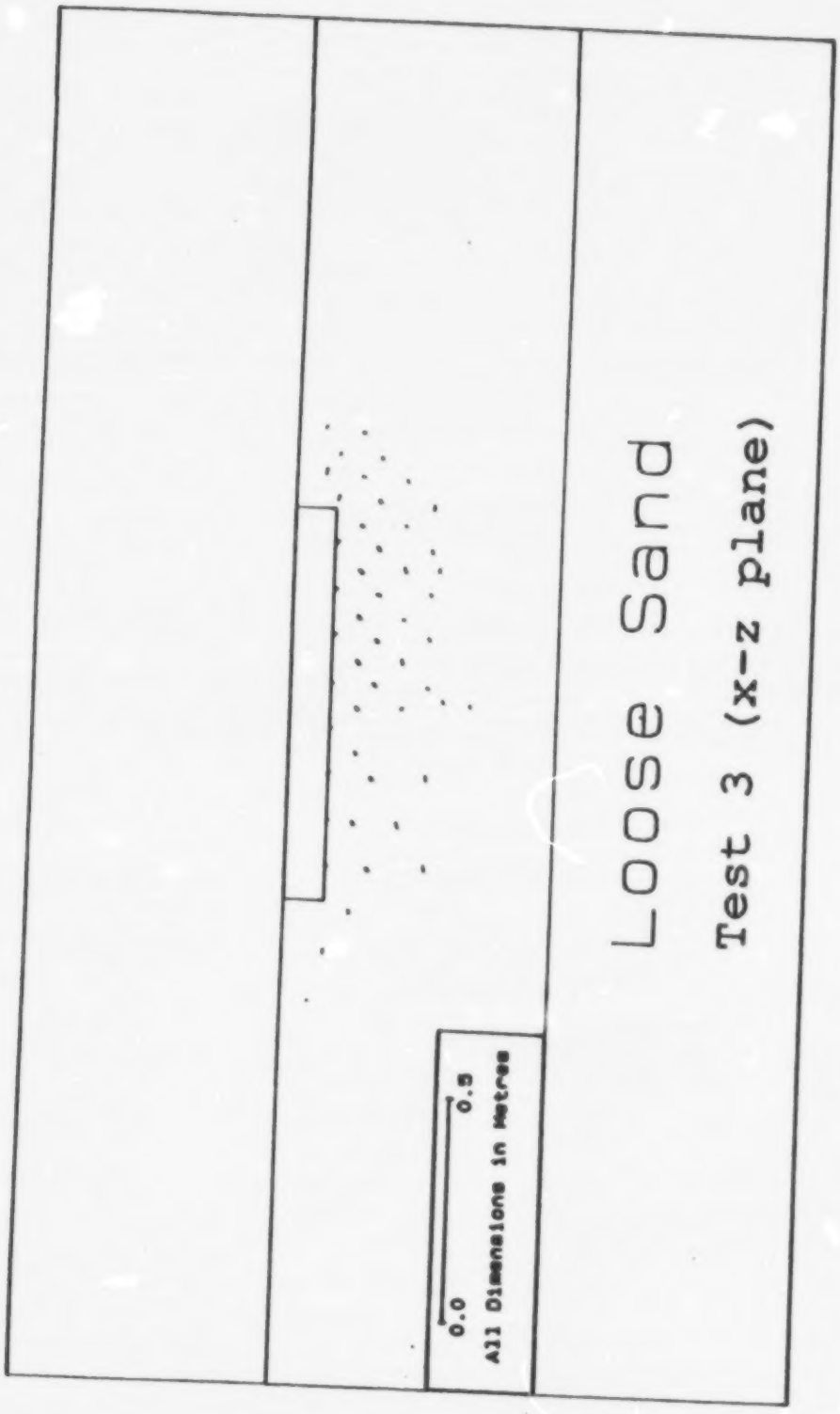

Figure 23a
Ball Displacements, Cross Sectional View
Scour Created Perpendicular to Page

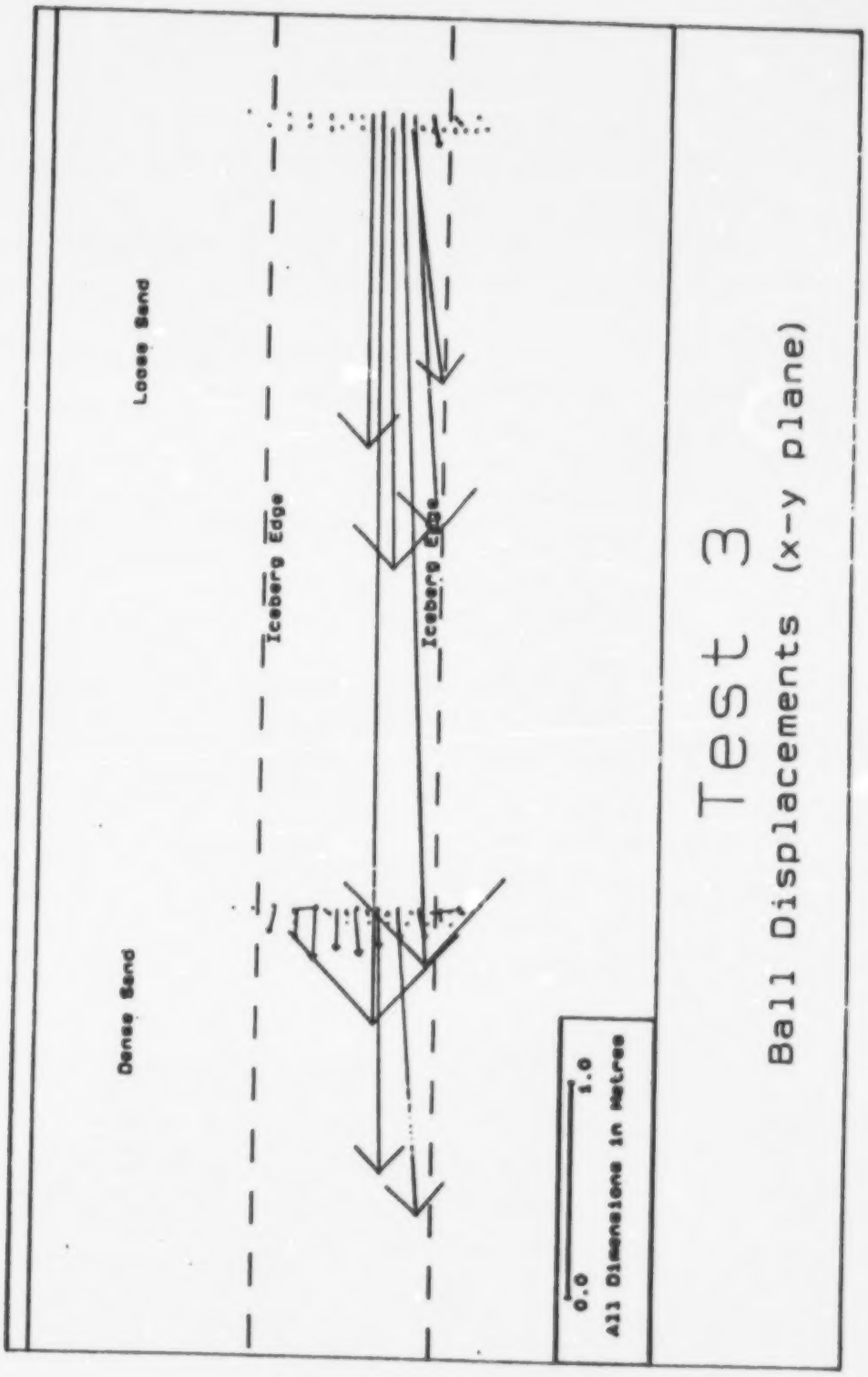

Figure 23b
Plan View
Scour Created from Left to Right

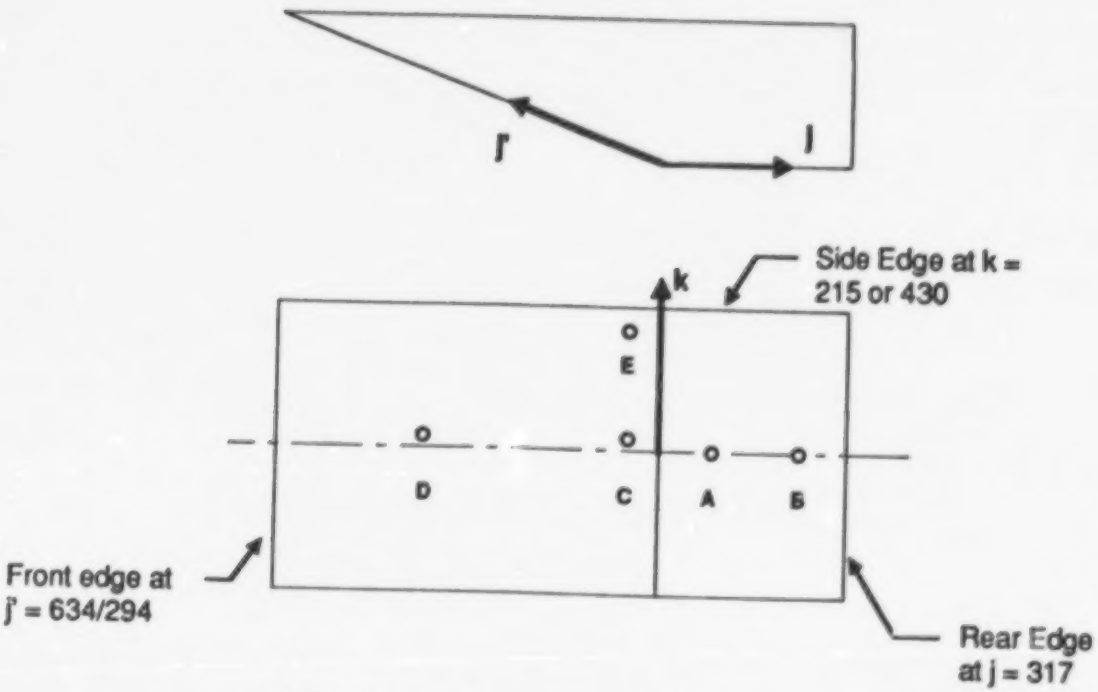

Cell	j	j'	k
A	55		0
B	205		0
C		85/75	40/38
D		280/255	40/38
E		85/75	150/160

Figures separated by slashes refer to coordinates in 15°/30° attack angle icebergs. All dimensions in mm.

Figure 24
Coordinate System on Iceberg and Pressure Cell Locations

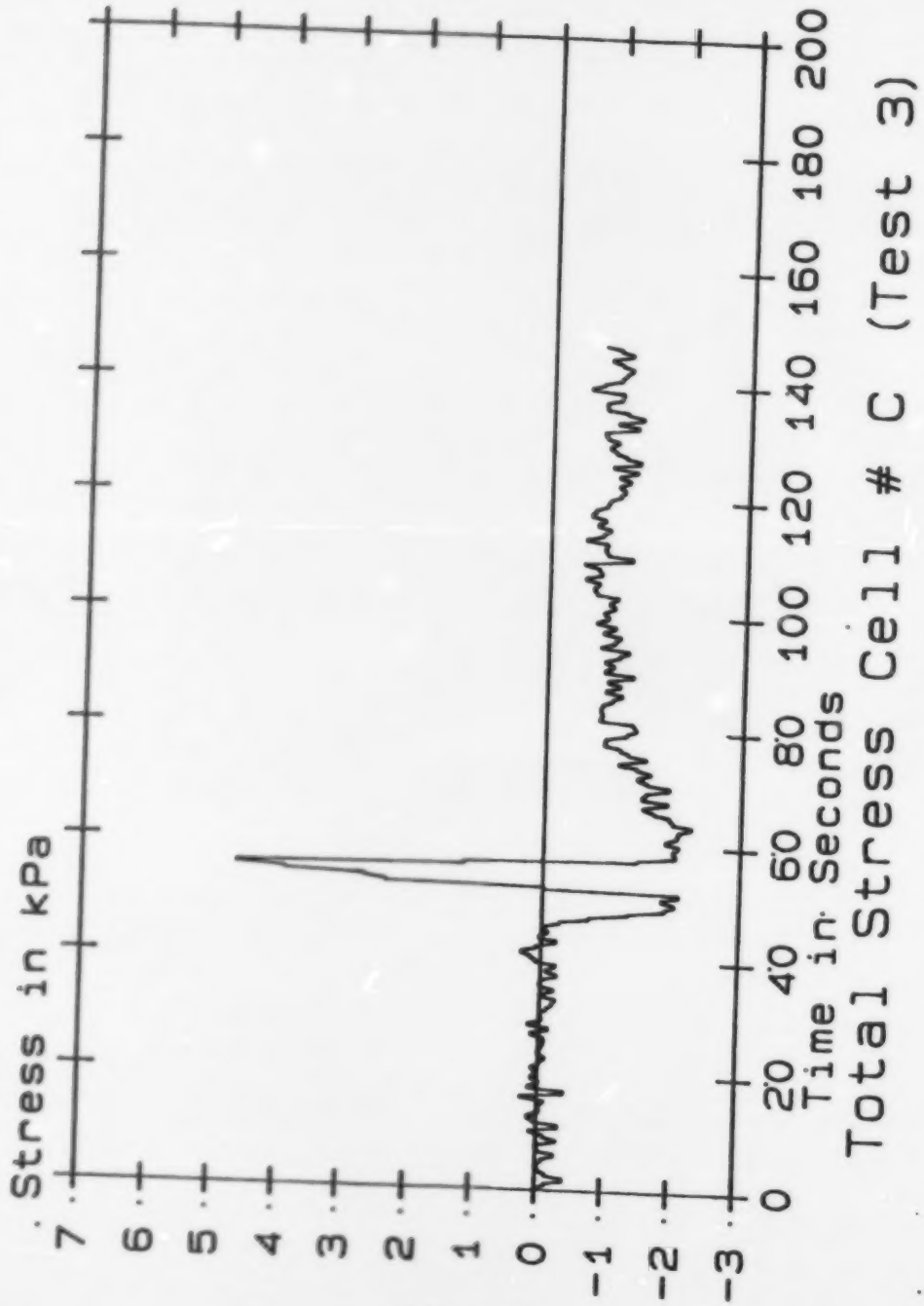

Figure 25
Total Stress on Horizontal Plane 75mm Below Scour Centreline

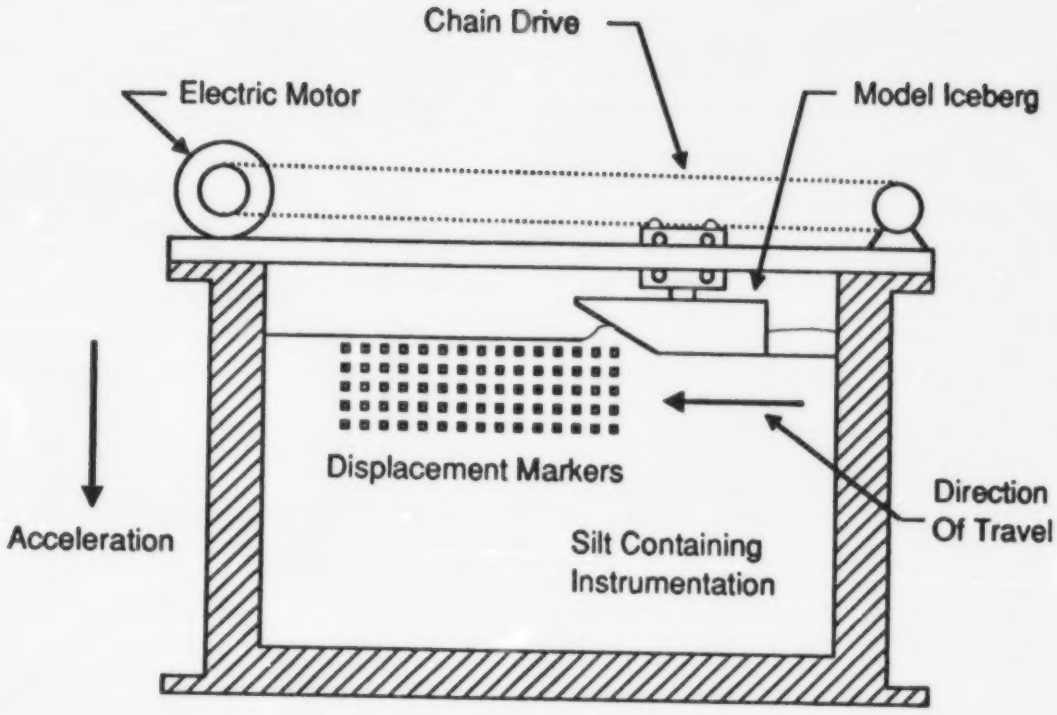

Figure 26
A Possible Centrifuge Model to Investigate Ice Scour